

THE SUMMER DISTRIBUTION OF TUNA IN RELATION TO THE GENERAL OCEANOGRAPHIC CONDITIONS OFF CHILE AND PERU**

Eliseo SANDOVAL T.*

CONTENTS

1. INTRODUCTION	23
2. ACKNOWLEDGEMENTS	24
3. DATA PROCESSING	24
4. OCEANOGRAPHIC CONDITIONS	25
5. HORIZONTAL CIRCULATION OFF CHILE AND PERU	28
Circulation	
6. DISTRIBUTION OF THE WATER MASSES ACCORDING TO CIRCULATION	30
7. GEOGRAPHICAL DISTRIBUTION OF THE SPECIES STUDIED	31
Geographical distribution by species	31
Distribution of species in relation to water masses	33
8. COMMENTS ON THE RECORDED CONDITIONS	34
9. LITERATURE CONSULTED	
FIGURES AND TABLES	

1. INTRODUCTION

The flow of the Pacific Ocean waters has been surveyed by various scientists, but the Southeastern Pacific area, especially off the coast of Chile, still remains only partially studied. This work gives a better insight into this area. Supplemented by additional data and observations gathered during the years 1962 to 1969, a clearer picture is provided that can be used in the future for the development of the different fisheries.

In this paper a study is made of the January-February-March distribution of temperature, salinity and oxygen, besides the geostrophic dynamics related to 500 decibars, from latitude 5°N and 50°S to a longitude stretching to 98°W along the coast of Chile, Peru and Ecuador. The distribution of the physical and chemical characteristics is closely related to the abundance of some marine species of tuna, such as yellowfin tuna (*Thunnus albacares*), albacore (*Thunnus alalunga*), bigeye tuna (*Thunnus obesus*), and striped marlin (*Tetrapturus audax*).

The Far Seas Fisheries Research Laboratory in Shimizu, Japan, kindly allowed the author to use the data and observations collected in cruises made aboard the R/V "Shoyo Maru" during 1962-63 and 1964-65, and of all the physical and chemical data obtained aboard the R/V "Kaiyo Maru" during the "Emerald" Expedi-

* Institute de Fomento Pesqueros, Santiago, Chile.

** Received December 20, 1970. Contribution No. 51 from Far Seas Fisheries Research Laboratory.

tion, carried out in Peruvian and Chilean waters between December 1968 and February 1969. Likewise, the United States National Oceanographic Data Center supplied some of the physical and chemical data gathered in 1960 during the "Deep Freeze" Expedition.

The Far Seas Fisheries Research Laboratory also gave the author every possible assistance so that he could, under the Japan Technical Cooperation Agency Scholarship Programme, study the distribution of tuna in the different seas, with special emphasis on the above mentioned area.

To this effect information was provided with regard to long-line fishing data from commercial Japanese vessels gathered during the summer months (January–February–March) between 1963 and 1967 (five years), plus data from the R/V "Shoyo Maru 1962–63 and 1964–65 cruises, and information gathered aboard the R/V "Azuma Maru" off the coast of Chile.

This paper was read at the 21st. Tuna Conference, held at the University of California, Lake Arrowhead, California, October 12–14th, 1970.

2. ACKNOWLEDGEMENTS

The author is most grateful to the Japanese Government for granting him, through the Overseas Technical Cooperation Agency, this scholarship, thus enabling him to study, at the Far Seas Fisheries Research Laboratory, the oceanographic conditions connected with the distribution of tuna. He also wishes to thank the staff at this Laboratory for supplying the background data used in writing this paper. He is indebted to Mr. Hajime YAMANAKA, Dr. Keiji NASU and especially to Dr. Ichiro YAMANAKA; and also to Mr. T. KAMIMURA and Dr. H. KAWAI of the Japan Seas Regional Fisheries Research Laboratory for their helpful criticism and advise. He also wishes to thank Dr. Michitaka UDA, Professor of Oceanography at Tokai University, for his valuable suggestions.

3. DATA PROCESSING

The oceanographic data were processed according to the usual technical methods. Figures were drawn with the horizontal distribution of temperature, salinity, oxygen and of geopotential surfaces at 0, 50, 100, and 200–decibar levels relative to a 500–decibar surface of no motion. Additional figures showing vertical distribution of temperature, salinity and oxygen were also drawn.

For the interpolation of physical and chemical values and calculation of geopotential dynamics relative to 500 decibars the computer at the Data Processing Center (Tokyo, Ministry of Agriculture and Forestry) was used.

Fishery data were processed according to the techniques described by Dr. Akira SUDA, Dr. Milner B. SCHAEFER and Dr. Susumu KUME in publications issued during 1965 and 1966–1969 respectively. Using these methods the following figures were

drawn for the 1963-1967 (five years) summer quarters (January-February-March) by one degree squares:

- a) Distribution of water masses with regard to the tuna catch distribution per degree of latitude and per 1,000 hook average, considering its distribution in ten degrees of longitude; and
- b) Total kilograms per degree of latitude, with regard to the average percentage per degree of longitude, considering its distribution in ten degrees of longitude. The catch rate per hook is given for every 1,000 hooks; in order to avoid decimals this value was multiplied by a factor of ten.

With regard to the area stratus in each case the rate of catch was computed by dividing the total catch per species by the number of hooks used.

4. OCEANOGRAPHIC CONDITIONS

From these graphs which refer to the horizontal distribution of summer values of temperature, salinity, oxygen and geopotential condition we can infer that the displacement of the subantarctic water mass in its surface limit occurs on an axis running in a southwest direction from the coast to an average latitude of 30° , considering for this boundary a temperature of about 19°C and a 34.3‰ salinity. To the south of this boundary a transitional zone is formed by the subtropical water mass at a point where the subantarctic water mass sinks (Figs. 2 and 3), moving then towards the north and under the surface.

On an axis which runs from an average latitude of 20° approaching the coast from the southwest we find the subtropical water, with a surface boundary temperature of 20°C and a salinity increasing from 34.5‰ to greater than 35.4‰ , and occupying approximately 50% of the surface in this zone. Just to the north, at 0° latitude, we find the tropical water mass with less than 34.0‰ salinity and a temperature increase from 24°C .

Upwelling areas appear to the south of these limits, and change in depth with the flow of the oceanic current.

Accordingly, both upwelling areas along the coast and the formation of similar areas in the edges of the highest flow rate are noticed. This condition is more noticeable in the 50 m. stratum (Figs. 4 and 5).

In the 50 m. depth level the distribution is the same, with some changes occurring in the equatorial area, where the predominance of tropical water decrease and the greater influence of subtropical water is observed, with a 5°C decrease in temperature as compared to surface water.

At this level the Peru-Chile Countercurrent, with a marked low oxygen content of less than 0.5 ml/L (Fig. 6), becomes quite evident near the coast of Chile and increases, due to the influence of the southern currents, to values higher than 5 ml/L as it approaches the open sea.

At a distance of 360 miles from the coast and a latitude of 33°S the oxygen content exceeds 6 ml/L, enveloping the Juan Fernandez Archipelago. This value stretches from the south, forming a tongue of water which reaches the 25°S latitude. In the equatorial area, southwest of the Galapagos Islands (Fig. 6), water with an oxygen content of less than 2 ml/L is observed due to the upwelling.

At the 100 m. level the subantarctic water lies 50 miles off the coast, in a tongue of water reaching 25°S in latitude, with a boundary of 34.3‰ salinity and a coastal limit of 14°C temperature. Here the transitional area is larger and the subtropical water is more diffused (Figs. 7 and 8).

The Peru-Chile Countercurrent (Fig. 9) is clearly seen spreading over a larger area, up to 37°S latitude. Farther away from the coast and as a part of the subantarctic waters the oxygen content exceeds 6 ml/L; 5 ml/L in subtropical waters.

In the equatorial area which lies southwest of the Galapagos Islands, the upwelling water stretches over a wider area and has a low oxygen content of less than 0.5 ml/L.

On the 200 m. level the subantarctic water mass with an 11°C temperature lies farther from the coast. The same 100 m. tongue of water, narrower and with a NE-SW inflection which is sharper than in the previous levels (Figs. 10 and 11), is still present. The subtropical water mass is distributed almost as it was at 100 m, although exhibiting a greater influence on the equatorial area, where the oxygen values increase to more than 1 ml/L. Here we find some centers with an oxygen content of less than 0.25 ml/L. These minimum values correspond to the displacement of the Peru-Chile Current towards the south east, and the Chile-Peru Current turning to the north and flowing away from the Chilean coast.

At this level the subsurface Peru-Chile Countercurrent is obviously well developed on a wide area off Peru (Fig. 12) and the northern coast of Chile, where it changes into a narrow strip which runs next to the coast up to a 37°S limit, and returns from this latitude in a WNW course with the prevailing oceanic current.

To the west of the Juan Fernandez Archipelago the subtropical water mass has a greater influence from a 200 m. depth towards the surface; this water mass has a temperature of over 15°C, and is widely spread due chiefly to the anticyclonic circulation. During the summer in the southeastern Pacific the greatest displacement and variation of this circulation are seen most intensely at approximately 42°S. The subantarctic water mass lies in the southern part, influencing the coastal area, moving somewhat separated from it because of the Peru-Chile Countercurrent which flows from an average latitude of 37°S along the coast and returns toward the WNW.

Distinct upwelling areas are observed around the equatorial area, especially within the 0-50 m. stratum. This upwelling is also evident along the coast of Peru and Chile, to an approximate 35°S latitude, greatly influencing the area's biological

productivity, thus creating the important pelagic resources found along the coast of Ecuador, Peru and Chile. In latitude 17°S and longitude 95°W , between 200 and 100 m., there is an upwelling which corresponds to an area also rich in pelagic resources (Fig. 45).

Profile I (Figs. 13 to 15) shows a strongly developed thermocline, occurring at a low depth between 3°S and 2°N , caused by the merging, at a low level, of subtropical, tropical and subantarctic waters. Over this thermocline is found subtropical water, with a temperature exceeding 16°C and a $>35\%$ salinity, associated to a >5 ml/L oxygen content.

The tropical water, with less than 34% salinity and temperature over 24°C associated to an oxygen exceeding 4 ml/L, is noticed distributed to the north of latitude 0° , towards a depth of about 50 m.

The subantarctic water, with a $<15^{\circ}\text{C}$ temperature and $<35\%$ salinity, is clearly observed under the discontinuity layer associated with a <4 ml/L oxygen level.

Between latitude 3°S and 1°N and from a 30 to 150 m. depth the South Equatorial Countercurrent (or Cromwell Current), with high temperature, salinity and oxygen content can be detected.

Profile II (Figs. 16 and 17) clearly shows the same distribution of water, except tropical water which is not seen in this profile.

The well-developed thermocline between latitude 16°S and longitude 90°W , with a 20°S latitude and 85°W longitude, lies at a minor latitude and due to the different upwelling areas is less developed towards the coast.

Profile III (Figs. 18 to 20) shows the same distribution as profile II, although the subtropical waters lie farther off the coast, and the thermocline is well developed from a 26°S latitude and a 81°W longitude toward latitude 19°S and 95°W longitude. Towards the southeast, due to the upwelling areas this thermocline is seen to be less developed than in profile II.

In profile IV (Figs. 21 to 23) the water mass distribution is similar to that of the previous profiles, though a transitional zone between the subtropical and subantarctic water mass, on 78° to 90°W longitude and a southwest direction, is clearly shown in the horizontal distribution. Due to this transitional area the thermocline between 90°W and the coast is less developed.

In profile V (Figs. 24 and 25) is noticed that most of this zone is covered by subantarctic water, sinking when it runs into low density water (46°S - 88°W), which moves toward the northwest driven by the current and the prevailing winds of the zone. This lower salinity water flows from the fiords to the subantarctic water mass during the whole year.

It is also possible to observe the divergence by this subantarctic water, which is divided into two branches, one of them moving toward the north, thus forming the Humboldt Current or Peru Oceanic Current. The other branch flows towards

the south, around Cape Horn, and forms the Malvinas Islands Current.

From profile VI to profile X (Figs. 26 to 30) can be detected the influence of the water from the Peru-Chile Countercurrent which is clearly developed near the coast at a 200 m. depth, except in profile IX (Fig. 29) where it changes under the greater influence of the subtropical water. Towards the south, in profile X (Fig. 30), the oxygen minimum which characterizes this countercurrent is divided into two parts: one with a < 0.25 ml/L minimum, near the coast, and the other with < 0.50 ml/L minimum, 200 miles off the coast.

The first part moves slightly farther south as part of the Peru-Chile Countercurrent, disappearing due to mixing, and the second one flows with the Chile-Peru Returning Current, which moves to the WNW from an approximate latitude of 37°S in the coast.

In profiles XI, XII and XIII (Figs. 31 to 33) the above-mentioned minimum does not exist, making this return toward the WNW more evident. These profiles clearly show the minimum salinity which prevails in this area and is produced by the persistent rainfall, characteristic of the southern channels zone (Table 2), and also by the corresponding river flow. This minimum, which together with the annual and seasonal fluctuations is a distinctive feature of the four seasons, moves toward the northwest, to an approximate 33°S latitude.

5. HORIZONTAL CIRCULATION OFF CHILE AND PERU

Using the data mentioned in part 1, graphs with the geostrophic dynamics related to a 500-decibar level of no motion, for 0, 50, 100 and 200 m. (Figs. 35 to 38) were drawn.

Since the Southeastern Pacific circulation off Ecuador has received special attention during recent years, this work gives general information about the horizontal circulation off Peru and Chile, up to a 50°S latitude.

This paper does not analyze the effects of the wind on the upwelling system which have a marked influence on the local upwelling system. It only studies the dynamics, separate from the effects of the prevailing winds, thus regarding the upwelling waters as waters which flow from depths not exceeding 100 m. near the coast.

This paper analyzes the general circulation in the Southeastern Pacific utilizing observations gathered over an extended time period and space. To estimate the horizontal dynamics it can be assumed that the conditions of the studied layers have no vertical motion. The effects of friction, strongly emphasized by CARRIER and ROBINSON (1962), as well as the wind-driven circulation along the coast are disregarded. These and other phenomena can be more precisely studied in smaller areas and shorter observation periods.

Circulation

Through several profiles the horizontal circulation shows that the convergence and divergence of Ekman layers occur along the coast of Peru and Chile. The location of these areas coincides with the areas of maximum force winds (BRANDHORST, 1963). Consequently, the coastal vertical movement from a <100 m. depth fits the vertical movement described by GUNTHER (1936) and WYRTKY (1963). This divergence is compensated by the high geostrophic convergence indicated in Figures 36 to 39, which clearly show those movements corresponding to the descriptions given by WOOSTER and GILMARTIN (1961), WYRTKY (1963), and BRANDHORST (1963) with regard to the coast of Peru and the northernmost coast of Chile.

Between 80° and 90°W and latitude 40°S a divergence occurs in the subantarctic waters, shaping a branch which advances to the north, creating the Peru Oceanic Current, also known as Humboldt Current. At latitude 8°S and 900 miles off the coast of Peru a divergence occurs in this Current, probably on account of the Equatorial Countercurrent, which in turn advances toward the northern coast of Peru and merges with the upwelling waters north of 15°S, a fact clearly detected in the geostrophic flow. The first branch of this divergence moves to the west, partly veering to the southwest. The second branch advances toward the coast and forms the surface Peru Countercurrent, which gradually returns to the northwest, turning finally towards the west, merging with the first branch and thus entering the South Equatorial Current.

Between 90° and 100°W the North Pacific Countercurrent flowing north of the Equatorial Countercurrent turns toward the southeast, and forms a branch which merges with the water circulation advancing to the southeast.

From about 90° and 100°W and 30° to 35°S a marginal, slow and clearly visible current moves northward (Table 1). Its features are low temperature, plus high salinity and oxygen content. As this current approaches a low latitude both its temperature and salinity increase, turning to the south and southwest and then toward the northwest, to a latitude of about 18°S between 93° and 100°W.

The subsurface Peru-Chile Current or Gunther Countercurrent, which can be detected in the 100-200 m. stratum, flows from the equatorial area to the south on a course near the coast of Peru and Chile. This southbound Countercurrent reaches its highest velocity near 100 m. (Table 1) and its widest breadth at 200 m., which gradually decreases between a 500 to 600 m. depth. The salinity and oxygen distribution shown in the profile running parallel to the coast (Fig. 34) coincides with the one described by WOOSTER and GILMARTIN (1961), and BRANDHORST (1963). This subsurface current flows up to a 37°S latitude and at this point is controlled by the seasonal and annual fluctuations. Close to this boundary it is absorbed by the northbound current, and thus returns to the equatorial area (Fig. 37).

The Peru Coastal Current, or Humboldt Current, which moves from the south and a 45°S latitude is caused by the divergence occurring in the Cape Horn Cur-

rent. This Current carries the aforementioned low salinity water which reaches the open sea from the channels and fiords. This low salinity water is carried to a latitude of approximately 33°S, near the south or southwest of the Juan Fernandez Archipelago, and its displacement toward these areas is subject to seasonal and annual fluctuations.

6. DISTRIBUTION OF THE WATER MASSES ACCORDING TO CIRCULATION

In order to analyze the water masses in the area of study, the author has drawn Figure 39, using data from ten stations distributed among the different currents. This figure shows the T-S curves and the oxygen content in various water masses.

Figure 39 indicates that the subantarctic water with a 34.3‰ salinity and a maximum surface temperature of 19°C, with an oxygen content of >5 ml/L to >6 ml/L in the nucleus, shows a surface penetration up to latitude 30°S, where it sinks and continues its subsurface displacement toward the north, influencing the coastal zone of Chile and Peru as far as a 15°S latitude (Figs. 35 and 36). This occurs in a layer of less than 100 m. near the coast and under the discontinuity layer, influencing only the upwelling water flowing toward said latitude, and far off the coast in areas where water upwells from deeper levels.

The subtropical water mass with high salinity >35.0‰, temperatures between 16°C and 20°C, and oxygen content of >5 ml/L covers most of the area. This water mass is pushed by the anticyclonic circulation from the subtropical area to the vicinity of the Chile-Peru coastline (Fig. 35), preserving in this area the existent high salinity and oxygen, thus contributing to a high biological productivity in the coastal areas of Chile and Peru.

The Equatorial Subsurface Countercurrent, or Cromwell Current, described by Knauss (1960) is produced by the inversion of the South Equatorial Current which moves toward the west pushed by the eastwinds, and which reverses its course between 20 and 40 m. depths. This causes a water accumulation in the equatorial area (170°W), creating a different level in the pressure gradient. Due to this, part of the South Equatorial Current, approximately between latitudes 2°S and 2°N, flows towards the east under this current from longitude 170°W. These waters, flowing east of the zone under study, sink progressively to a 400 m. depth. The nucleus of this countercurrent lies in a 140°W longitude, at a 100 m. depth, slowly ascending toward the surface as it approaches the South American Continent, reaching a depth of 20 m. below the surface in a 95°W longitude (Figs. 13, 14 and 15).

This nucleus is clearly visible west of the Galapagos Islands in Figures 35 to 38, which correspond to the geopotential dynamics. A branch of this South Equatorial Countercurrent flows into the Northern Hemisphere, and another branch shifts toward the southeast, reaching the coast of Peru under the Peru Oceanic Current

and modifying the characteristics of the waters upwelling north of 15°S, which show high temperature and salinity values and also a high oxygen content.

The low-salinity tropical or equatorial water can be detected north of the subtropical water, in a thin 50 m. layer, clearly shown in the T-S curve of Station 233 (Fig. 39). This thin layer of high-salinity subtropical water mixes with the subantarctic water below, forming an intermediate layer between both water masses, with salinities from about 34.6‰ to 34.9‰, and temperatures ranging between 9° and 14°C. This layer has a distribution in depth varying between 50 and 600m., reaching its widest breadth at a 200 m. depth. This water mass, called Subsurface Equatorial Water by Wyrtky, remains for a long time in the equatorial area, keeping a minimum oxygen content of <0.5 ml/L and <0.25 ml/L in its nucleus.

This same water mass, with such a low oxygen content and relative high salinity and temperature, is also detected off the coast of Peru and Chile, as can be seen in the T-S curve of Figure 39. Some of this water flows to the Southern Hemisphere and merges with the Subsurface Peru-Chile Current, or Gunther Current, which moves towards the south, to a 37°S latitude. From this point it returns to the north following the general anticyclonic circulation, as seen in Figure 38, showing the geopotential topography at 200 m. (related to 500 decibars).

7. GEOGRAPHICAL DISTRIBUTION OF THE SPECIES STUDIED

The distribution of hook rates during the southern summer months of January, February and March over a 5-years period (1963-67) for each of the four species is represented in Figures 40 to 43. The average catch for all hooks appears in the same one degree squares that correspond to their respective hook rates.

From these figures the author can infer that at present the greatest fishery corresponds to bigeye tuna in terms of catch in kilograms, followed accordingly by the yellowfin tuna, the albacore tuna and striped marlin (Table 3). As seen in Figure 40 the fishery of albacore tuna has been rather poor due to its geographical distribution. In general, the fishing grounds for these species lie north of 20°S and between 90° and 80°W longitude. The waters south of this area have scarcely been exploited, as shown in Figures 40 to 43. Figure 41 clearly shows that the fishing effort is almost nil in an area where the albacore is one of most important species.

Another important species found in the same area is the southern bluefin, specimens of which were caught by the R/V "Shoyo Maru" during an exploratory cruise carried out in 1963.

Geographical distribution by species

a) Bigeye tuna (*T. obesus*)

The bigeye tuna has been intensively exploited up to 10°N, except in the northern winter months of January, February and March, and along the northwestern

border (130°W). It is estimated that these fish are the extension of a densely distributed group feeding along the North Pacific Current (KUME and JOSEPH, 1969).

The equatorial area, from 10°N to 20°S, has also been intensively exploited since the long-line fishery began in the Eastern Pacific Ocean (SUDA, SCHAEFER, 1965). A comparison between the hook rates of SUDA and SCHAEFER (1965) and KUME and SCHAEFER (1966) shows that the high abundance areas lie between the Galapagos Islands (Fig. 41) and the Ecuadorean seacoast, especially in the first annual quarter. This high abundance is also evident toward the west of the Galapagos Islands to 115°W, distributed as far as a 38°S latitude, though south of 20°S and from 100°W to the east this species has been barely exploited during the first quarter. The abundance during the first and fourth quarters, south of 20°S, shows a seasonal migration toward the south during the southern summer months.

b) Yellowfin tuna (*T. albacares*)

During the second and first quarters of the year the yellowfin tuna is abundantly found in an area stretching from 6° to 12°N, east of 120°W and in the area spreading between 0° and 8°N, and from 105°W to 115°W (KUME and JOSEPH, 1969). This species is also abundant east of 115°W to the Ecuadorean coast and in a 3° band south of the Equator (Fig. 42). South of this area the abundance is good, though it is included in a long low-capture area. A second abundance band is found diagonally between 3° and 19°S, and between 105° and 90°W.

Another area of relative abundance is detected during the first quarter in the south, near the Juan Fernandez Archipelago.

c) Albacore tuna (*T. alalunga*)

During the third quarter of the year, the albacore tuna is distributed in the southern area on two zone bands, spreading in an east-west direction, as confirmed by KUME and SCHAEFER (1969). These bands are of less importance than the ones found in the first quarter. The north zone band, centralized around 16° to 20°S during the first quarter, is located more to the north during the second and third quarters.

During these quarters (KUME and SCHAEFER, 1969) a southern band stretching between 25°S and 30°S can be easily assessed through the catch rate per hook. It is obvious that during the first quarter these bands reach the surveyed area, showing that the north band, between 16° and 20°S, extends to 40°S.

It is quite possible that the gathering towards the north (between 20° and 30°S) of these high abundance bands during the third quarter of the year, as described by KUME and SCHAEFER (1966), is related to the oceanographic changes influencing the fish migration from areas lying farther to the south.

d) Striped marlin (*T. audax*)

The fishery of this species provides a great deal of information, showing that its distribution is widely extended across the Eastern Pacific Ocean. There are

some areas, though, where this species is found in greater abundance. The first area, lying in the equatorial region (3°N to 4°S and 87° to 95°W), has a high hook rate (Fig. 43). The second area lies between 10° and 16°S , and from 90° to 100°W . This last distribution, extending during the first annual quarter between 90° and 100°W , shows as in the above-mentioned cases a minimum fishing effort.

Distribution of species in relation to water masses

a) Bigeye tuna (*T. obesus*)

The distribution of bigeye tuna during this quarter, in which the anticyclonic gyre is in its southern limit, reaches a south latitude boundary of 38°S . Figures 44A and B show quite an even distribution, although three heavy catch areas, as estimated per average hook and per kilogram, are evident.

The first area lies between 2° and 3°S , the second between 20° and 22°S , and the third between 29° and 32°S , though the latter reveals a minimum hook effort, as compared to the other two areas. Bigeye tuna, according to its distribution along the schematic profile, can be found along a transitional water front which corresponds to the merging of subantarctic and tropical waters, with $>15^{\circ}\text{C}$ temperatures, and salinities higher than approximately 34.5‰. The more important groups are located in the vicinity of the upwelling areas (Figs. 44A and B).

b) Yellowfin tuna (*T. albacares*)

Subject to seasonal changes, this is one of the species which shows a highest movement with regard to the position of the thermocline. During its juvenile stage the yellowfin tuna is commonly found near islands (KAWAI, 1969), as is the case of the group found near the Juan Fernandez Archipelago, located at an approximate latitude of 33°S and 80°W . Apparently this group migrates in the first annual quarter toward that area from its spawning grounds searching for food. Its distribution could be located in tropical and sub-tropical waters at a low depth, in temperatures $>19^{\circ}\text{C}$ and in waters with a high oxygen content $>4\text{ ml/L}$.

c) Albacore tuna (*T. alalunga*)

This species was always found near areas of transitional waters. It is believed that the albacore move at a depth close to the transitional water zone with a high oxygen content. Figures 44A and B show two important catch groups, remarkable for their catch both per average fish percentage and per kilogram. The first group is found between 15° and 20°S at the upwelling zone latitude described above. This group is in its adult stage. The second group, located more to the south, is in the juvenile stage (H. YAMANAKA, 1969) and lives near the surface in the transitional zone.

d) Striped marlin (*T. audax*)

This species is generally distributed within the tropical and subtropical waters. Its southern limit is the transitional water zone. Two main groups are found in its distribution: one around tropical waters, and another in subtropical waters. A

third group of less importance is detected in the transitional zone. Based on this fact one can presume that the striped marlin moves above the transitional zone, near upwelling waters with temperatures $>16^{\circ}\text{C}$ and salinities $>34.5\text{‰}$ (Eigs. 44A and B).

8. COMMENTS ON THE RECORDED CONDITIONS

1. Up to latitude 15°S the upwelling waters in the coast are influenced by the contribution of subantarctic water. In southern summer, the limit of the upwelling water system is 35°S . South of this latitude and near the coast the subantarctic water is distributed from the surface to deep levels.

North of 15°S the upwelling system is influenced by the contribution of subsurface waters from the Equatorial Undercurrent also known as the Cromwell Current.

2. The influence of the Peru-Chile Countercurrent or Gunther Countercurrent reaches latitude 37°S off the coast of Chile. This Countercurrent with a low oxygen content is sometimes displaced beyond 41°S . From 37°S it returns towards the equatorial area, thus increasing the minimum oxygen content in a larger area off the coast of Chile, Peru and Ecuador. Off Peru and Ecuador this minimum has a wider breadth, stretching over an approximate surface of 9,600 square miles, at a 200 m. depth, maintaining such a minimum in the surveyed area due to the circulation system.

An intrusion of the North Equatorial Countercurrent on these waters would create the phenomenon known as "El Niño". This intrusion will cause the waters of the Peru-Chile Countercurrent to move beyond 37°S and closer to the surface, exerting a wider interference on the surface waters, thus forcing the Peru Coastal Current to the west. It is evident that the observations of the seasonal and annual fluctuations of the southern boundary (Lat. 37°S) of this subsurface current, and at the same time meteorological observations of the trade winds in the Southern and Northern Hemispheres would facilitate predicting the appearance of "El Niño". This phenomenon is caused by a decrease in the south and southwest winds, combined with an increase of the trade winds from the Northern Hemisphere, creating the necessary conditions for the expansion of the transequatorial circulation of the North Equatorial Countercurrent, which flows to the Ecuadorian and Peruvian coast. This increased transport effects a higher displacement towards the south which frequently reaches Chile.

3. The minimum salinity recorded over an area next to the coast, which normally is displaced toward the north to approximately 33°S latitude, is formed in the channel and fiord zone due to the rains that prevail in this area (Table 2) and the resulting fluvial contribution, which in enclosed areas (Isla Apiao) forms 6‰ salinities on an approximately 0.5 m. layer. These waters leave the channel zone

and mix with the subantarctic surface waters carried to the north by the current which can be detected in the geopotential topography. Through mixing, this minimum finally disappears.

4. West of the Peru Oceanic Current, a cold current of subtropical water is displaced to the south equatorial area. This northward displacement increases its temperature and salinity. At 12°S latitude, this current veers to the south and southwest, thus creating conditions that promote biologically favorable conditions due to the upwelling waters formed at a 200 to 100 m. depth, mainly in the vicinity of 20° S and 92°W.

5. East of the Galapagos Islands, on a 50 m. stratum and over a minimum oxygen, there is high biological productivity, which is created by high oxygenation and high water temperature caused by water flowing from the subsurface South Equatorial Countercurrent and the surface Peru Countercurrent. Excellent areas for the fishing of bigeye tuna and striped marlin are common up to approximately 15°S latitude. This is also seen toward the northwestern side of the Galapagos Islands, between 90°W and 100°W. South of this area there are also excellent fishing grounds, specially near the previously described upwelling in subtropical waters. Their distribution is limited to the south by transitional waters and toward the east by the returning Chile-Peru Current, whose main characteristic is a low oxygen content.

It is quite evident that in its mature stage albacore tuna (*Thunnus alalunga*) are found distributed over the open sea, specially with regard to subtropical waters in upwelling areas located approximately at 20°S and 92°W. On the other hand, immature specimens are found in transitional waters, south of 30°S, at depths limited to the east by waters with a low oxygen content, as described above.

6. The yellowfin tuna (*Thunnus albacares*) is found in tropical and subtropical waters of high surface productivity, and in shallow upwelling waters in the open sea.

7. Usually in the open sea the distribution of high tuna concentrations coincides with the areas of highest upwelling waters located in subtropical and tropical waters, at levels showing a high oxygen content. The distribution of the species studied in this paper is limited by transitional waters formed by the merging of subtropical and subantarctic waters, and especially to the east by waters of low oxygen content flowing from the Chile-Peru Current. This fact can be ascertained by comparing the figures which correspond to the horizontal distribution and the average distribution per percentage of hooks used with the total catch weight per species over the schematic distribution of water mass.

8. Figure 45, showing the average hook rate of tuna and striped marlin from December 1968 to February 1969 for every five degree square, is given as supplementary data. This distribution confirms the position and highest hook rates in areas which correspond to upwelling waters near the coast and in the open sea.

9. For a better display of the water position Figure 46 shows the distribution of water mass at 100 m. depth, the main upwelling waters and gives also the general prevailing currents from a 0 m. depth, and the location of the areas with highest yield in the long-line tuna fishery.

LITERATURE CONSULTED

- BENNETT, E. 1963. An Oceanographic Atlas of the Eastern Tropical Pacific Ocean, based on data from Eastropac Expedition. October-December 1955. *Bull., Vol. VIII (2). Inter-Amer. Trop. Tuna Comm.*
- BJERKNES, J. 1961. "El Niño" study based on analyses of ocean surface temperatures, 1935-57. *Bull. Vol. 5 (3). Inter-Amer. Trop. Tuna Comm.*
- BLACKBURN, M. 1961. Distribution and Abundance of Eastern Tropical Pacific Tunas in Relation to Ocean Properties and Features. *Man. Inf. Pacific Tuna Conf. Honolulu, 1961, V, (4).*
- . 1962. Tuna Oceanography in the Eastern Tropical Pacific. *U. S. Dept. Int. Fish and Wildlife Spec. Rep. Fish. N° 400.*
- . 1965. Oceanography and the Ecology of Tunas. *Oceanogr. Mas. Biol. An. Rev., 3.*
- BOGOROV, V.G. 1967. Productive regions of the ocean. Original title: *Produktionye raionyok-eana.* From: *Prioroda, 1967, N° 10.*
- BRANDHORST, W. 1963. Descripción de las condiciones oceanográficas en las aguas costeras entre Valparaíso y el Golfo de Arauco, con especial referencia al contenido oxígeno y su erlación con la pesca. *Ministerio de Agricultura. Dirección de Agriculturay Pesca. Santiago, Chile.*
- GROMWELL, T. 1958. Thermocline Topography, Horizontal Current and "Ridging" in the Eastern Tropical Pacific. *Bull. III (3), Inter-Amer. Trop. Tuna Comm.*
- GUNTHER, E.R. 1936. A report on oceanographical investigations in the Peru Coastal Current. *Discovery Reports 13.*
- FORSBERGH, E. D. and W. BROENKOW. 1965. Oceanographic Observations from the Eastern Ocean Collected by the R/V Shoyo Maru, October 1963-March 1964. *Bull. Vol. X (2), Inter-Amer. Trop. Tuna Comm.*
- KAMIMURA, T. and M. HONMA. 1963. Distribution of the yellowfin tuna *Neothunnus macrop-terus* (Temminck and Schlegel) in the tuna longline fishing grounds of the Pacific Ocean. *Report of Nankai Regional Fisheries Research Laboratory No. 17, 1963.*
- KAWAI, H. 1969. On the Relationship between Thermal Structure and Distribution of Longline Fishing-Grounds of Tunas in the Intertropical Atlantic-I. Analysis Based on Isotherms on Level Surfaces, Topographies of Thermocline, etc. No. 2, *Bull. Far Seas Fisheries Research Laboratory No. 2 Shimizu, Japan.*
- KNAUSS, J. A. 1960. Measurements of the Cromwell Current. *Deep-Sea Res., Vol. VI, (4), Inter-Amer. Trop. Tuna Comm.*
- KUME, S. and S. JOSEPH. 1969. The Japanese longline fishery for tunas and bullfishes in the Eastern Pacific Ocean east of 130°W. 1964-1966. *Inter-Amer. Trop. Tuna Comm. Bull. XIII (2).*
- KUME, S. and M. B. SCHAEFER. 1966. Studies on the Japanese longline fishery for tuna and

- marlin in the Eastern Tropical Pacific Ocean during 1963. *Bull. XI (3), Inter-Amer. Trop. Tuna Comm.*
- . 1969. Ecological studies on bigeye tuna V. A critical review on distribution, size-composition and stock structure of bigeye tuna in the North Pacific Ocean (North of 16°N). *Bull. Far Seas Fisheries Research Laboratory*. No. 1, Shimizu, Japan.
- NAKAMURA, H. and H. YAMANAKA. 1962. Relation between the distribution of tunas and the ocean structure. *Jour. Oceanogr. Soc. Jap.* 15 (3).
- . 1969. Tuna distribution and migration.
- NASU, K. 1969. Current of Peru. (in Japanese). *La mer Tome 7* No. 1.
- REID, J.L. 1961. On the geostrophic flow at the surface of the Pacific Ocean with respect to the 1000-decibar surface. *The Johns Hopkins Press. Baltimore* No. 1.
- . 1965. Intermediate waters of the Pacific Ocean. *The Johns Hopkins Press. Baltimore*, No. 2.
- SHIOHAMA, T. 1969. A note on the marlins caught by tuna longline fishing in the Eastern Pacific Ocean east of 130°W. *Bull. Far Seas Fisheries Res. Lab.* No. 1.
- SUDA, A. and M.B. SCHAEFER. 1965. General review of the Japanese tuna longline fishery in the Eastern Tropical Pacific Ocean 1956-62. *Inter-Amer. Trop. Tuna Comm., Bull. IX (6)*.
- SUDA, A., S. KUME and T. SHIOHAMA. 1969. An indicative note on a role of permanent thermocline as a factor controlling the longline fishing ground for bigeye tuna. *Bull. Far Seas Fisheries Research Laboratory*. Shimizu, Japan. No. 1.
- STOMMEL, H. 1963. Summary charts of the mean dynamic topography and current field at the surface of the ocean, and related functions of the mean wind stress. *Massachusetts Institute of Technology Cambridge, U. S. A. Studies on Oceanography*.
- SVERDRUP, H. V., M. W. JOHNSON and R. H. FLEMING. 1969. *The Oceans*. Prentice-Hall, New York. Eighth printing, 1969.
- TUREKIN, K. 1968. *Oceans*. Prentice-Hall, Englewood Cliffs, New Jersey, USA.
- WOOSTER, W. and T. CROMWELL. 1958. An oceanographic description of the Eastern Tropical Pacific. *Bull. Scripps. Instn. Oceanogr. Univ. Calif.* (7).
- and M. GILMARTIN. 1961. The Peru-Chile Undercurrent. *Vol. XIX (3). Scripps. Instn. Oceanogr. Univ. Calif.*
- WYRTKY, K. 1963. Total integrated mass transports and actual circulation in the Eastern South Pacific Ocean. *Vol. VIII. Scripps. Instn. Oceanogr. Univ. Calif.*
- . 1965. Surface Current of the Eastern Tropical Pacific Ocean. *Inter-Amer. Trop. Tuna Comm. Bull IX (5)*.
- YAMANAKA, H. and N. ANRAKU 1965. Surface Currents in the Indian Ocean as seen from drift of tuna longline gear. *Report No. 22. Nankai Regional Fisheries Research Laboratory*. No. 22.
- , J. MORITA and N. ANRAKU. 1969. Relation between the distribution of tunas and water types of the North and South Pacific Ocean. *Bull. Far Seas Fisheries Research Laboratory*. No. 2 Shimizu Japan,

夏季におけるチリー・ペルー沖の一般海況と マグロ分布との関係

エリゼオ・サンドバル

本研究では、チリー・ペルーおよびエクアドルに沿う沿岸域から 98°W に至る海域の、5°N から 50°S にわたり、南半球の夏（1—3 月）における水温・塩分および溶存酸素量の分布ならびに 500 デンパーを基準面とした地衡流について検討した。そして、その海況とマグロおよびカジキの分布との関係についても検討した。

15°S までの沿岸域における湧昇流は亜南極水の影響を受けており、そして南半球の夏季における湧昇域は 35°S が南限となっている。そして、15°S 以南および沿岸水域では亜南極水塊が表層から深層にまで分布しており、さらに 15°S 以北の湧昇流はクロムエル海流として知られる赤道潜流に起因した次表層水の影響を受けている。

ペルー・チリー反流（ギュンター反流）の影響はチリー沿岸沖の 37°S まで達しているが、溶存酸素量の少ないこの反流は 41°S 以南に達することがある。なお、その反流は、37°S から赤道域へ流れており、酸素量はチリー・ペルーおよびエクアドル沖にわたる広範な水域において高くなっている。

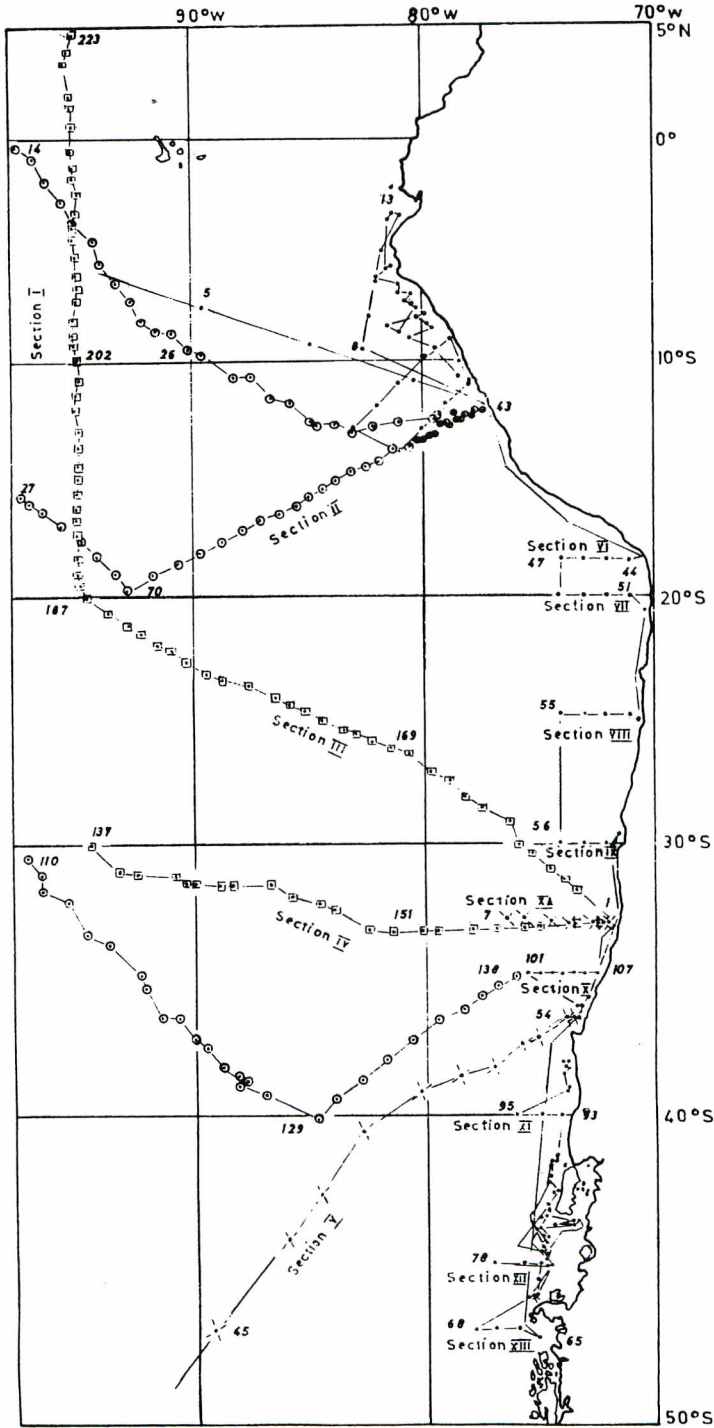
さらに、この海域における北赤道反流の流入はエル・ニーニョ（“El Niño”）として知られており、この現象はペルー・チリー反流に起因しているものと考えられ、37°S 以南にまで達している。

ペルー沖合流の西方においては亜熱帯系水塊が南部赤道域へ輸送されており、その輸送過程で水温・塩分ともに高くなっている。そして、12°S においてこの流れは南および南西へ流向が変わっており、複雑な流動が好漁場構成の要因となっているようである。また、20°S、92°W 付近の 100—200 m 層において時計廻りの渦流域が認められ、その海域は低温高かんとなっている。

この海域におけるメバチマグロおよびマカジキの好漁場は、およそ 5°N—15°S までに認められ、またガラパゴス諸島北西方向の 90°W—100°W にもみられている。このガラパゴス諸島海域の南では、特に 20°S、90°W の湧昇域が好漁場となっており、これらの好漁場は南側で移行水域（Transitional water）；東側で酸素量の低いチリー・ペルー海流の逆流（Returning Chile-Peru Current）と接している。

そして、成熟したビンナガマグロは沖合水域に分布し、特に 20°S、92°W の 200 m 層における低温かん域と好漁場が一致している。一方、未成熟群の漁場は概して 30°S 以南の移行水域に認められ、さらにキハダマグロの漁場は熱帯および亜熱帯域の浅い湧昇域にみられている。

FIGURES AND TABLES



R/V "Glacier" (Deep Freeze) January-March, 1960
 R/V "Shoyo Maru" December-February, 1962-1963
 December-February, 1964-1965
 R/V "Kaiyo Maru" December-February, 1968-1969

Fig. 1. Track and oceanographic stations mentioned in the text.

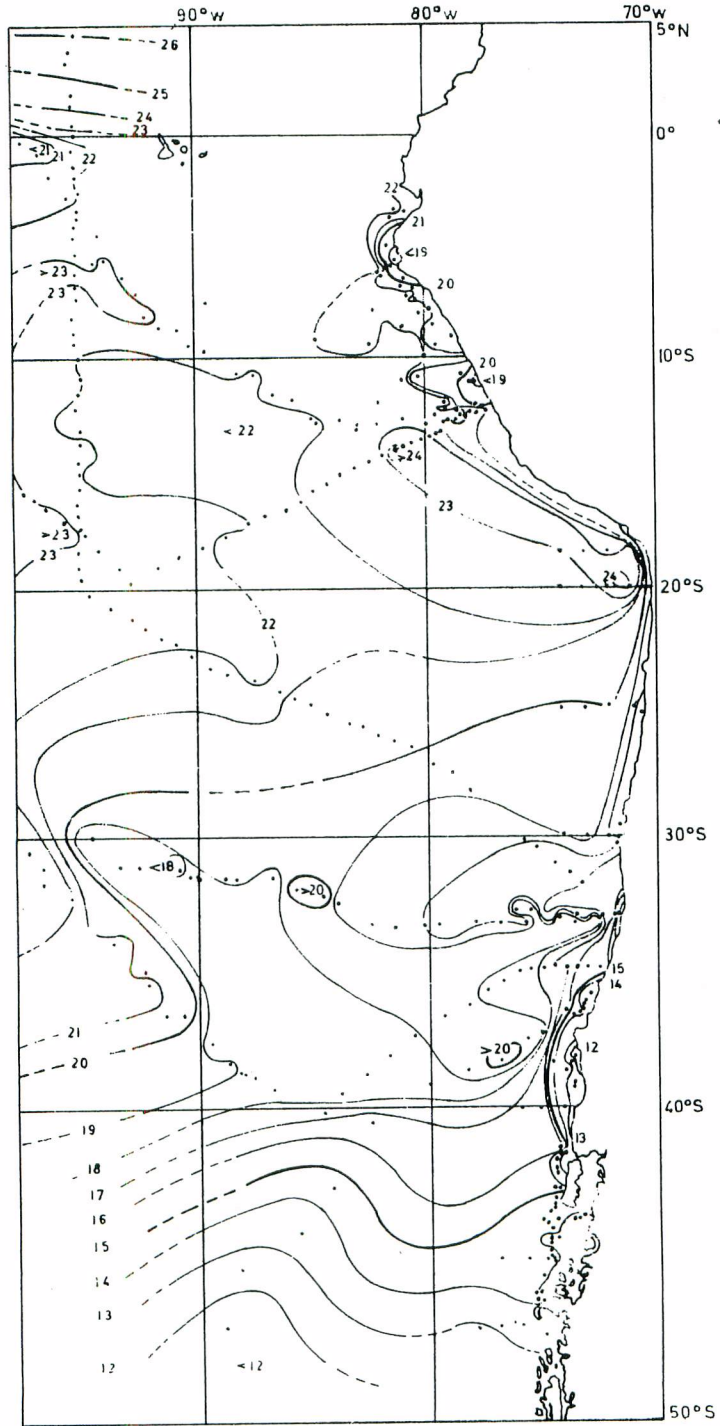


Fig. 2. Temperature distribution ($^{\circ}\text{C}$) at 0 m.

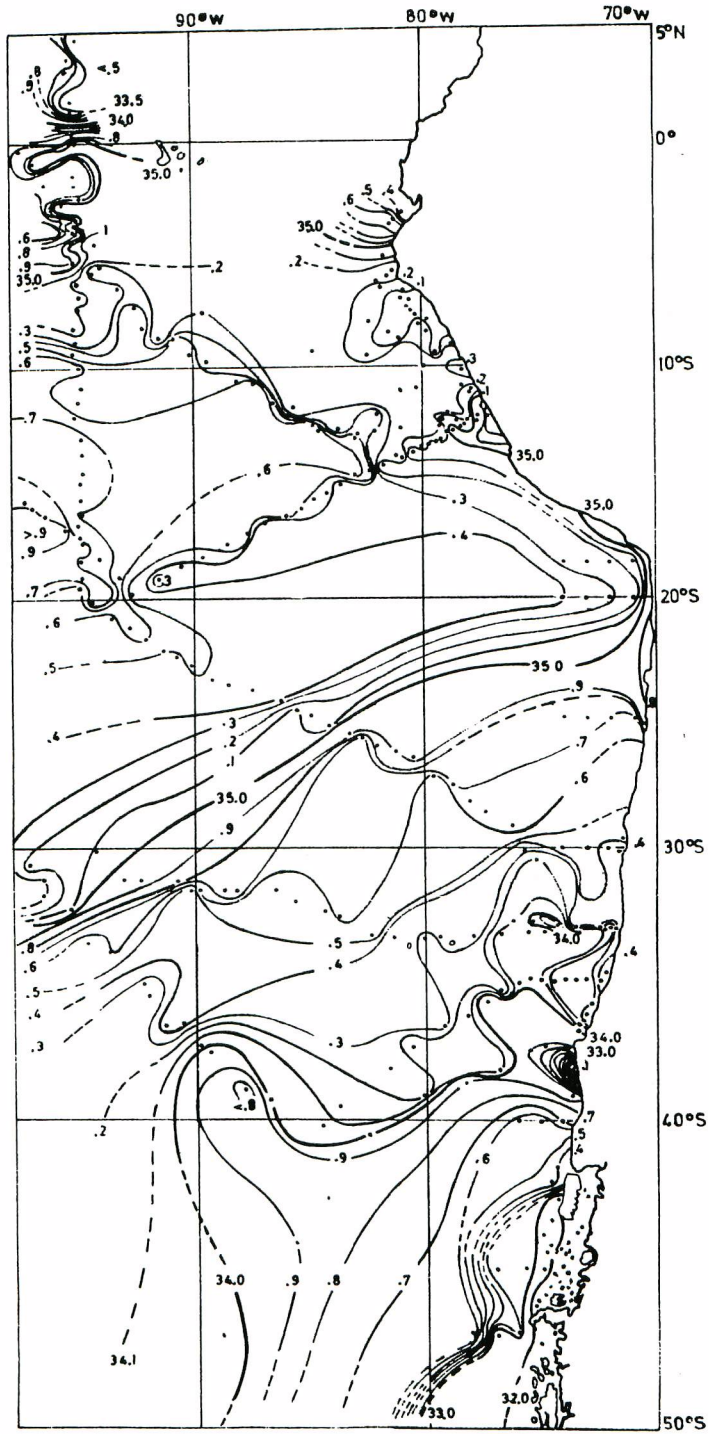


Fig. 3. Salinity distribution (‰) at 0 m.

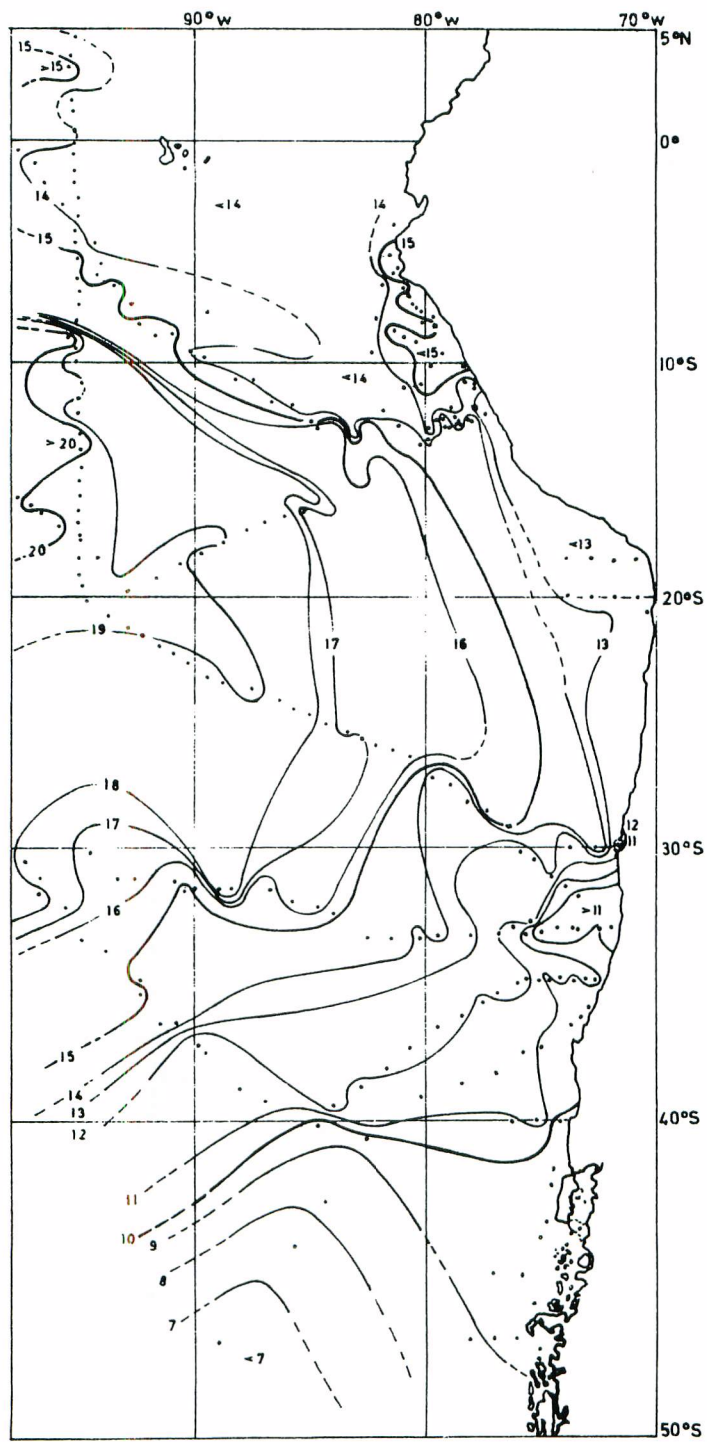


Fig. 4. Temperature distribution ($^{\circ}\text{C}$) at 50 m.

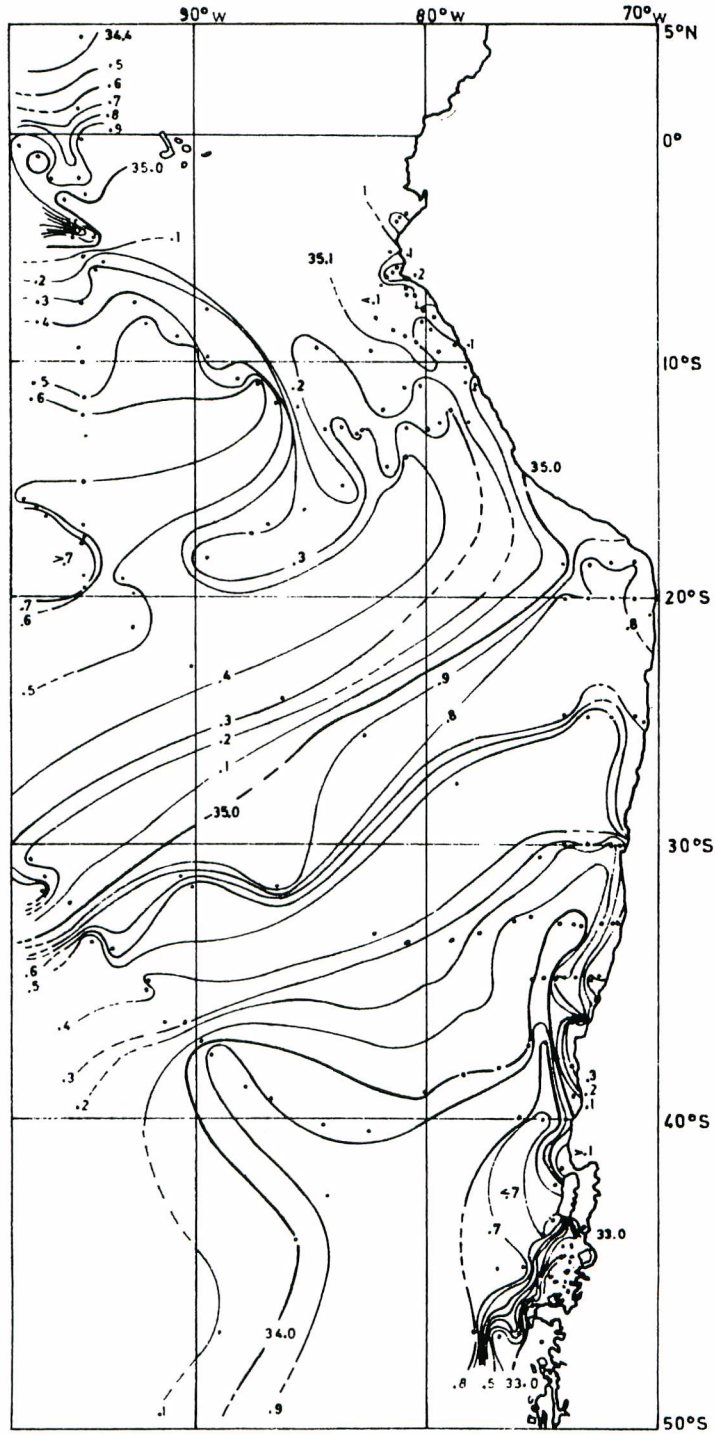


Fig. 5. Salinity distribution (‰) at 50 m.

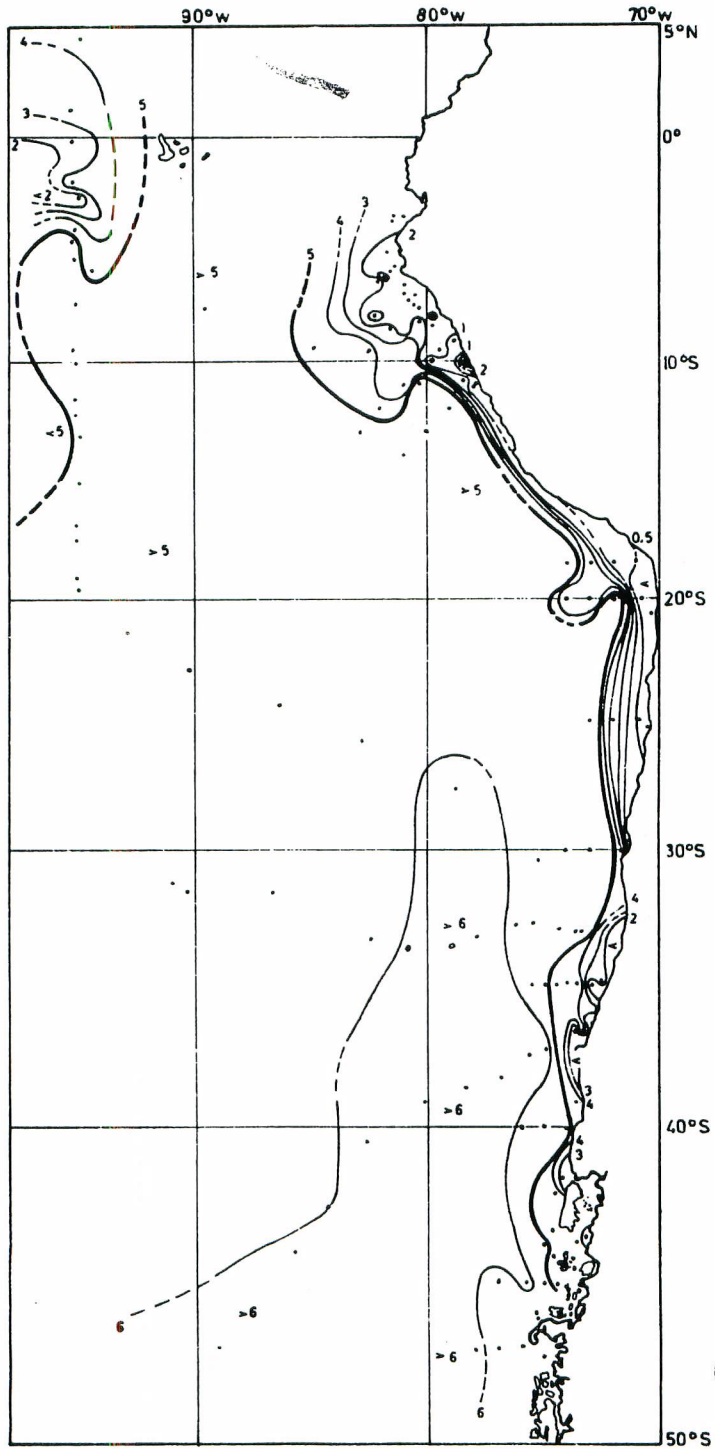


Fig. 6. Oxygen distribution (ml/L) at 50 m.

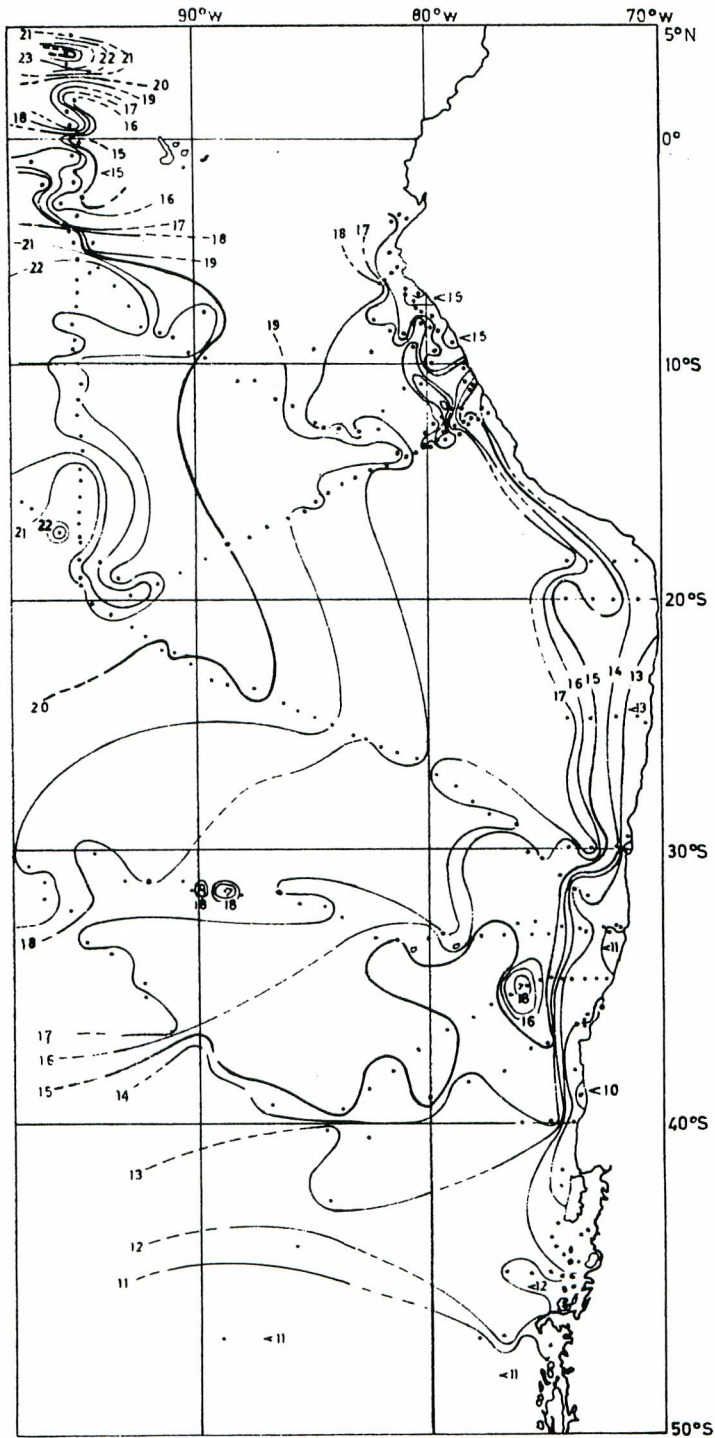


Fig. 7. Temperature distribution (°C) at 100 m.

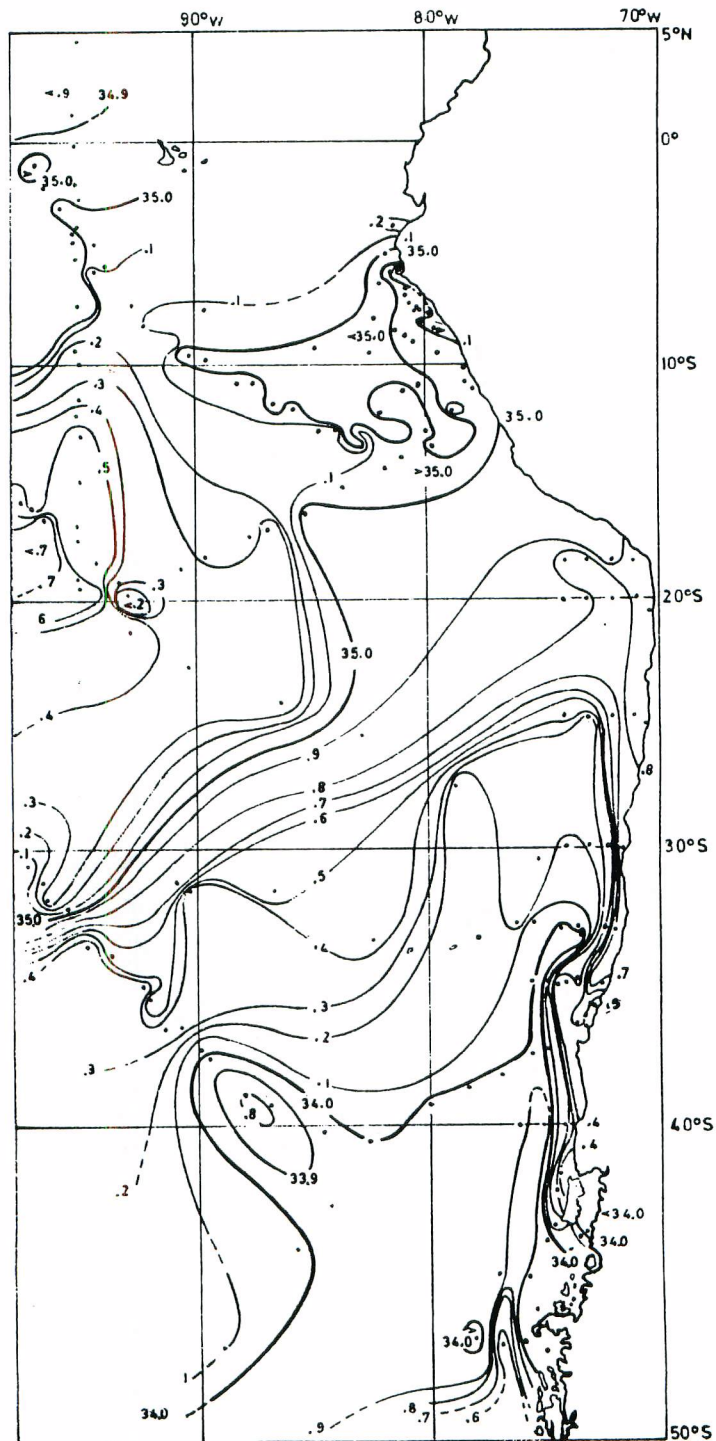


Fig. 8. Salinity distribution (‰) at 100 m.

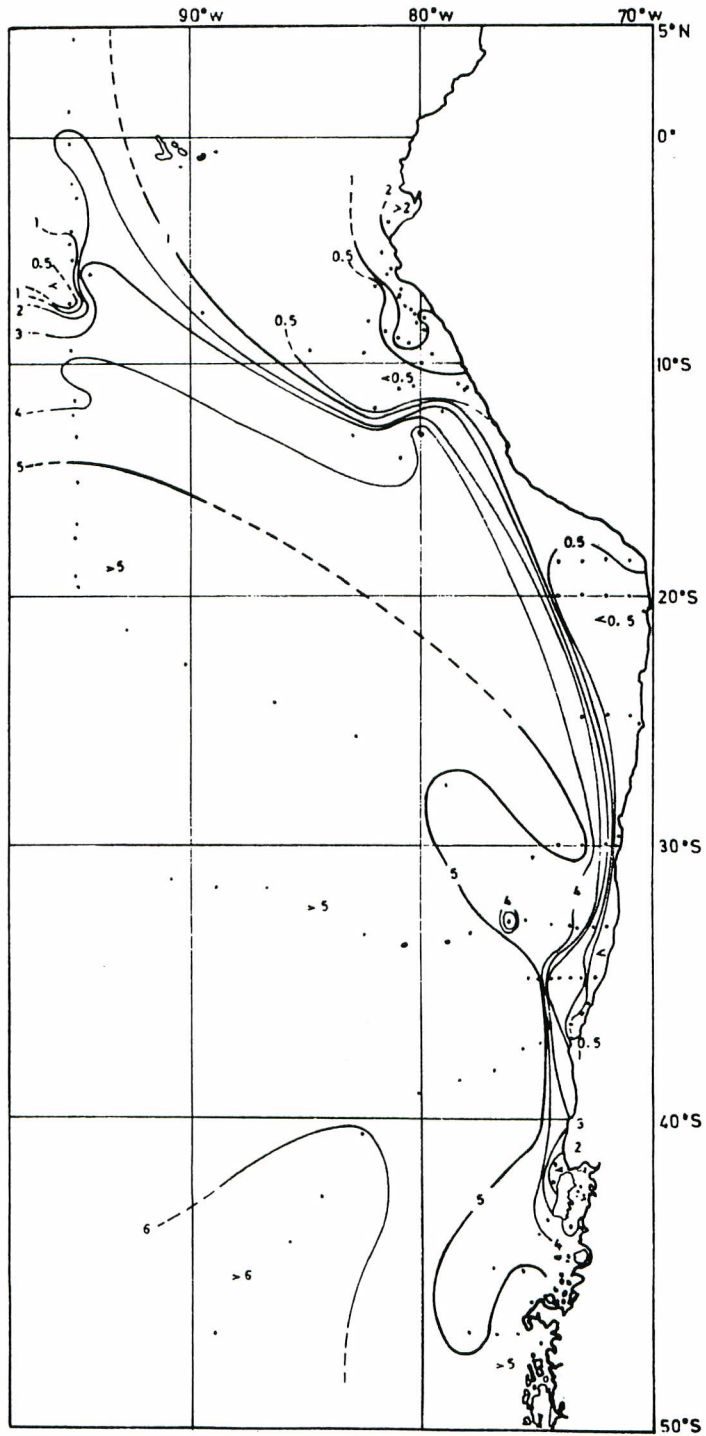


Fig. 9. Oxygen distribution (ml/L) at 100 m.

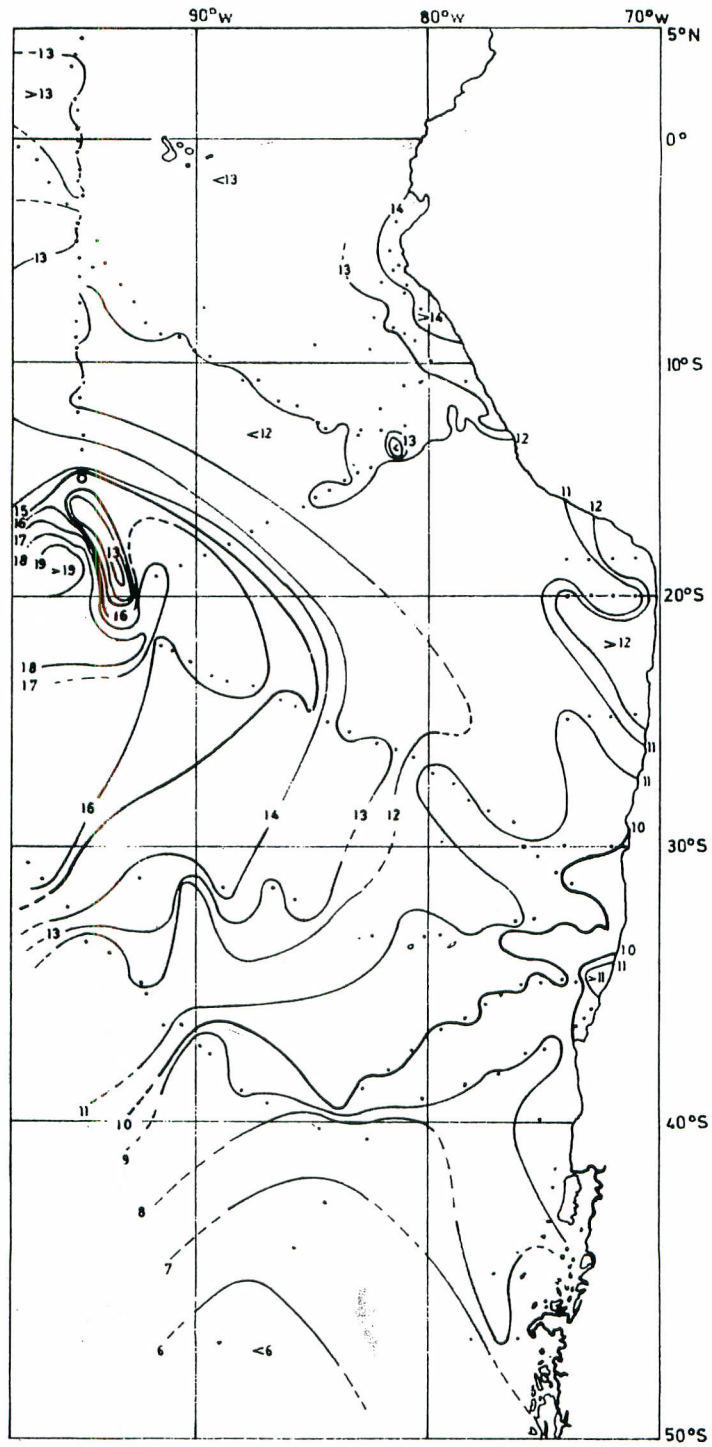


Fig. 10. Temperature distribution ($^{\circ}\text{C}$) at 200 m.

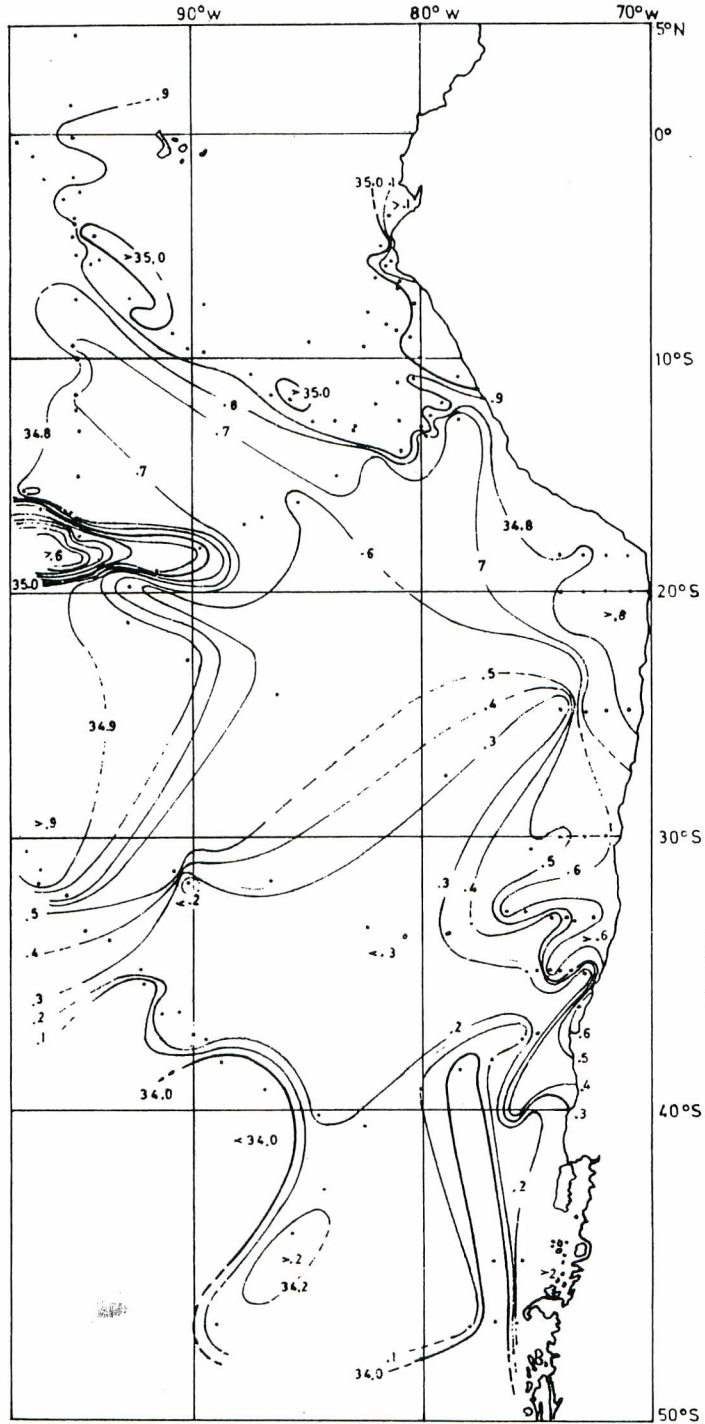


Fig. 11. Salinity distribution (‰) at 200 m.

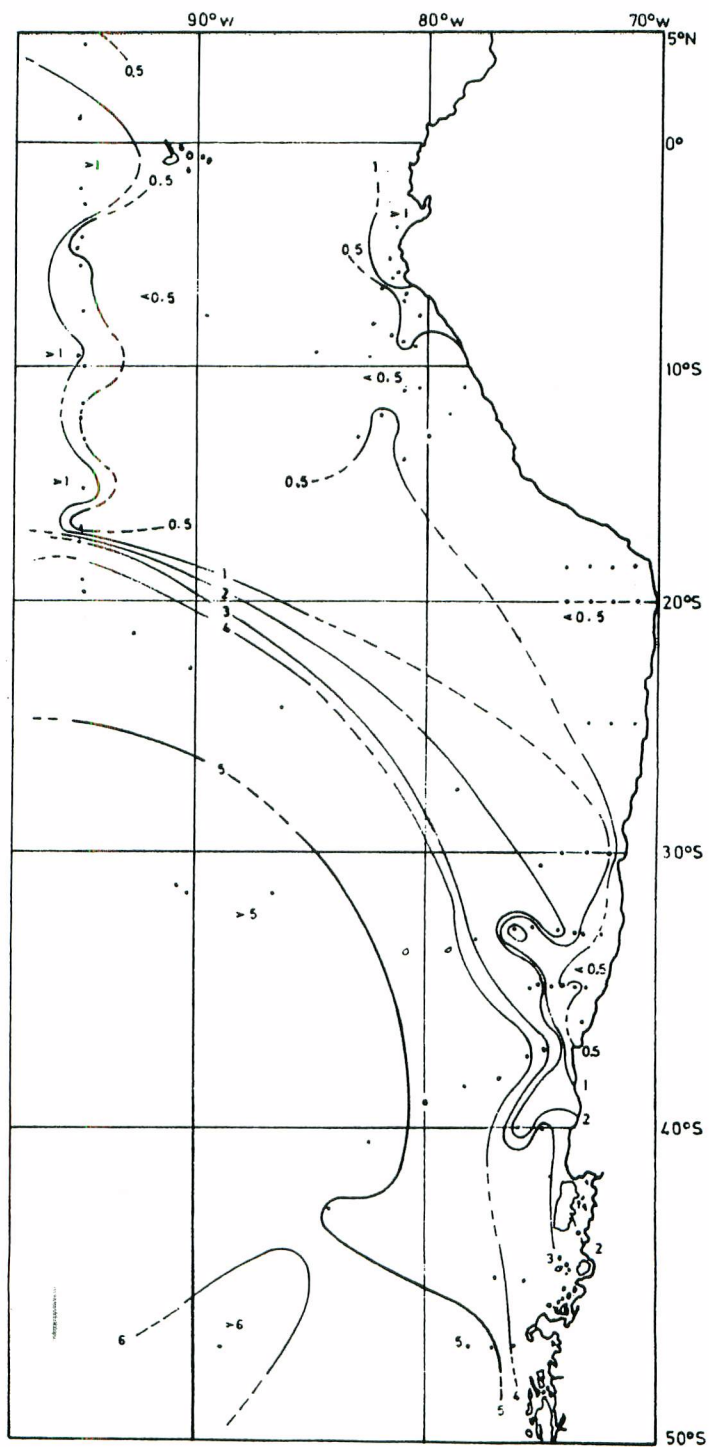


Fig. 12. Oxygen distribution (ml/L) at 200.

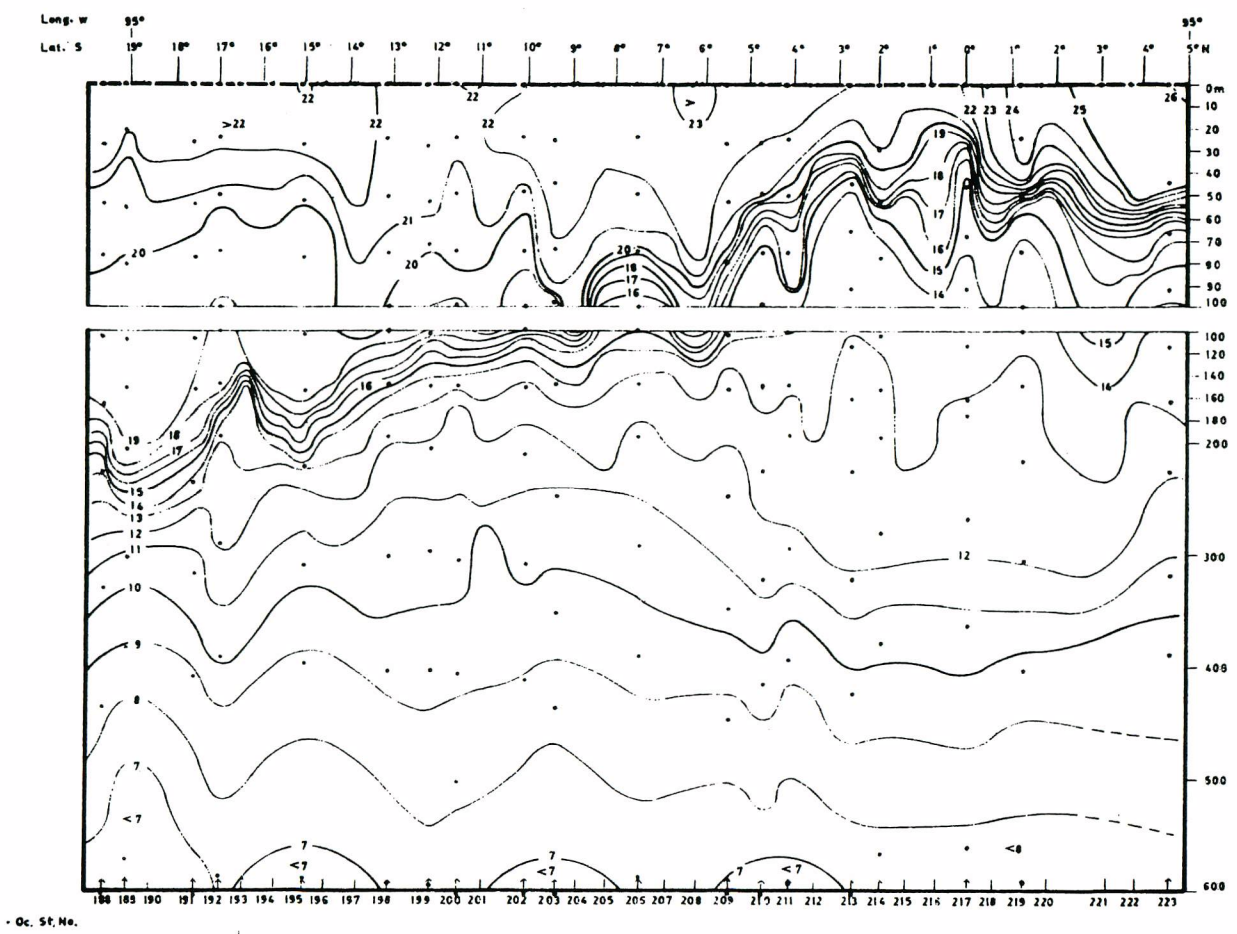


Fig. 13. Temperature profile (°C) along section I.

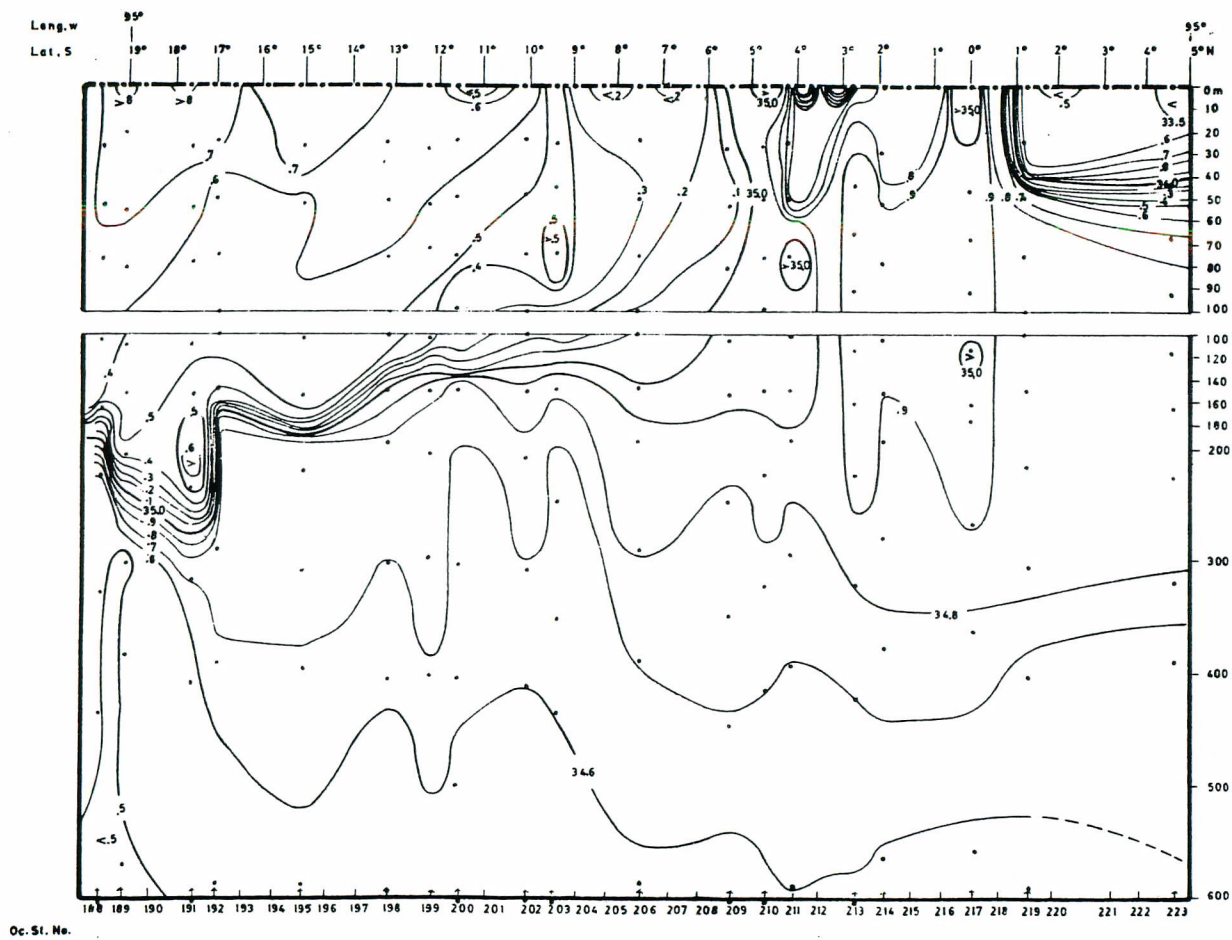


Fig. 14 Salinity profil (%) along section I.

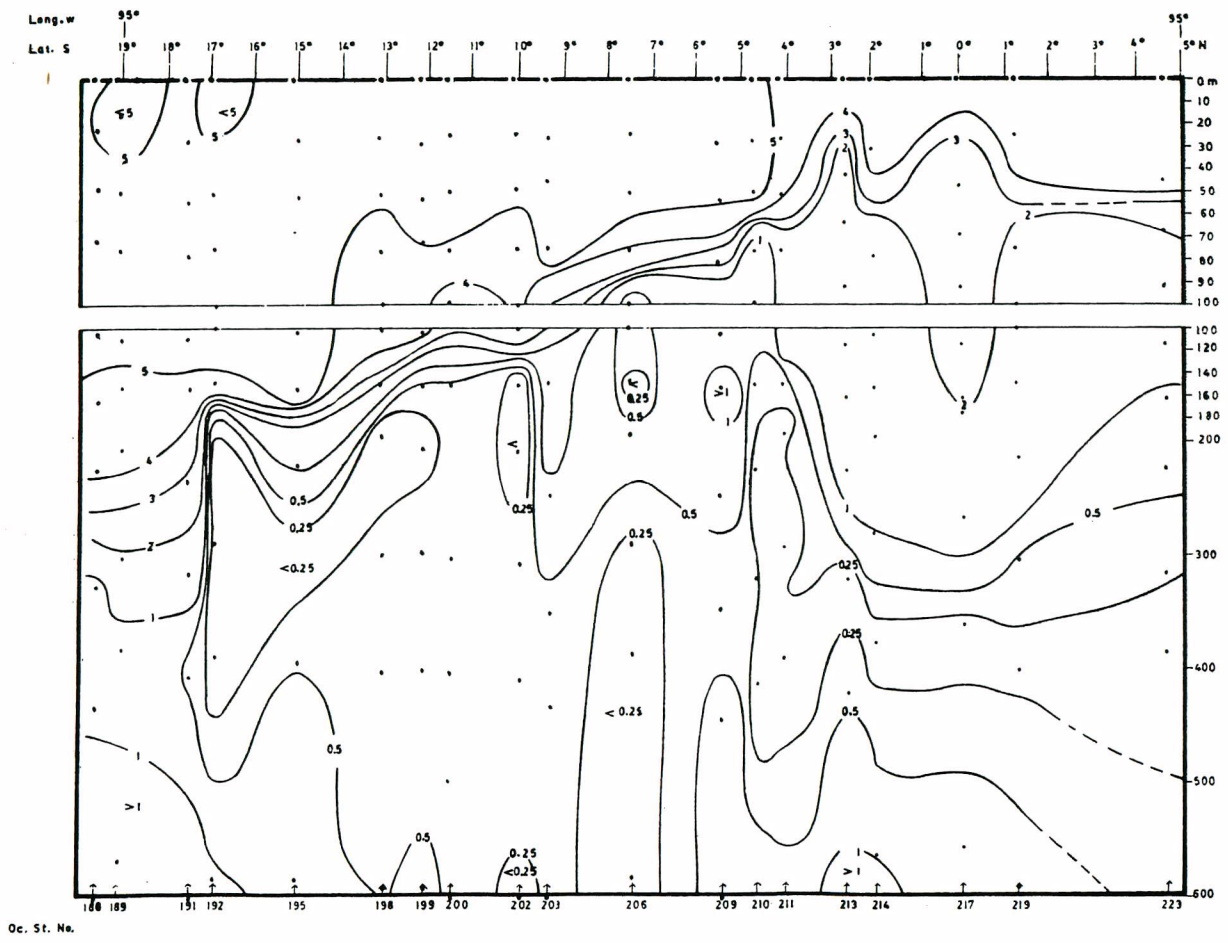


Fig. 15. Oxygen profile (ml/L) along section I.

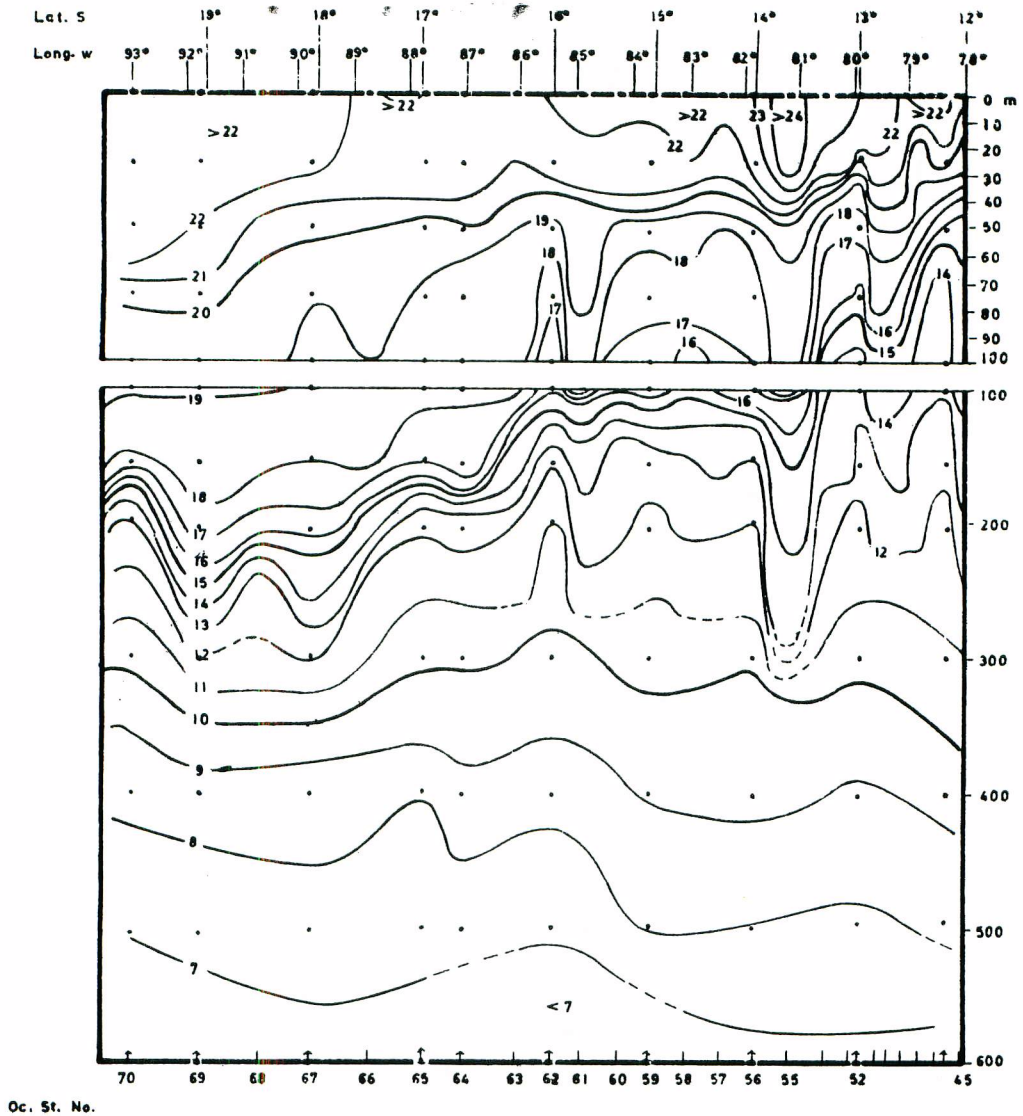


Fig. 16. Temperature profile ($^{\circ}\text{C}$) along section II.

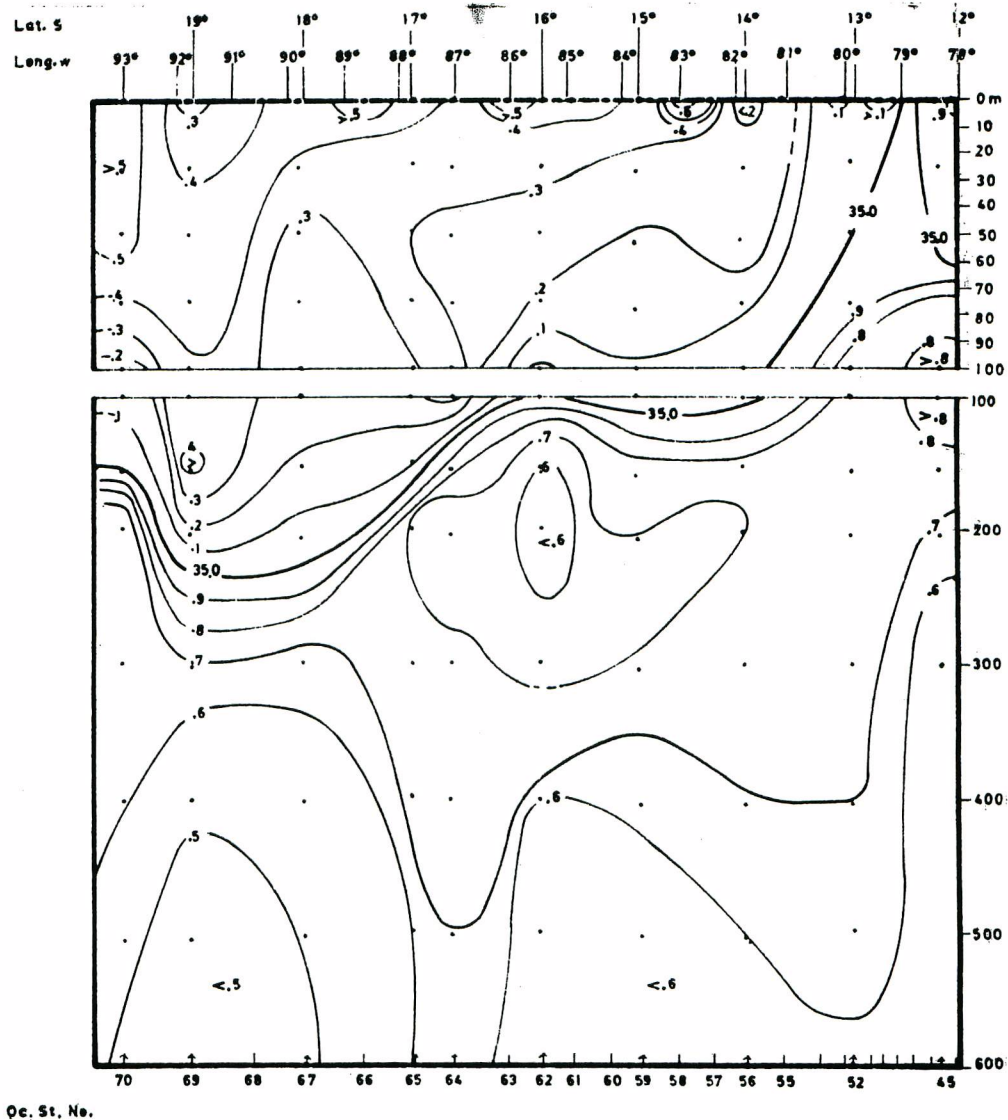
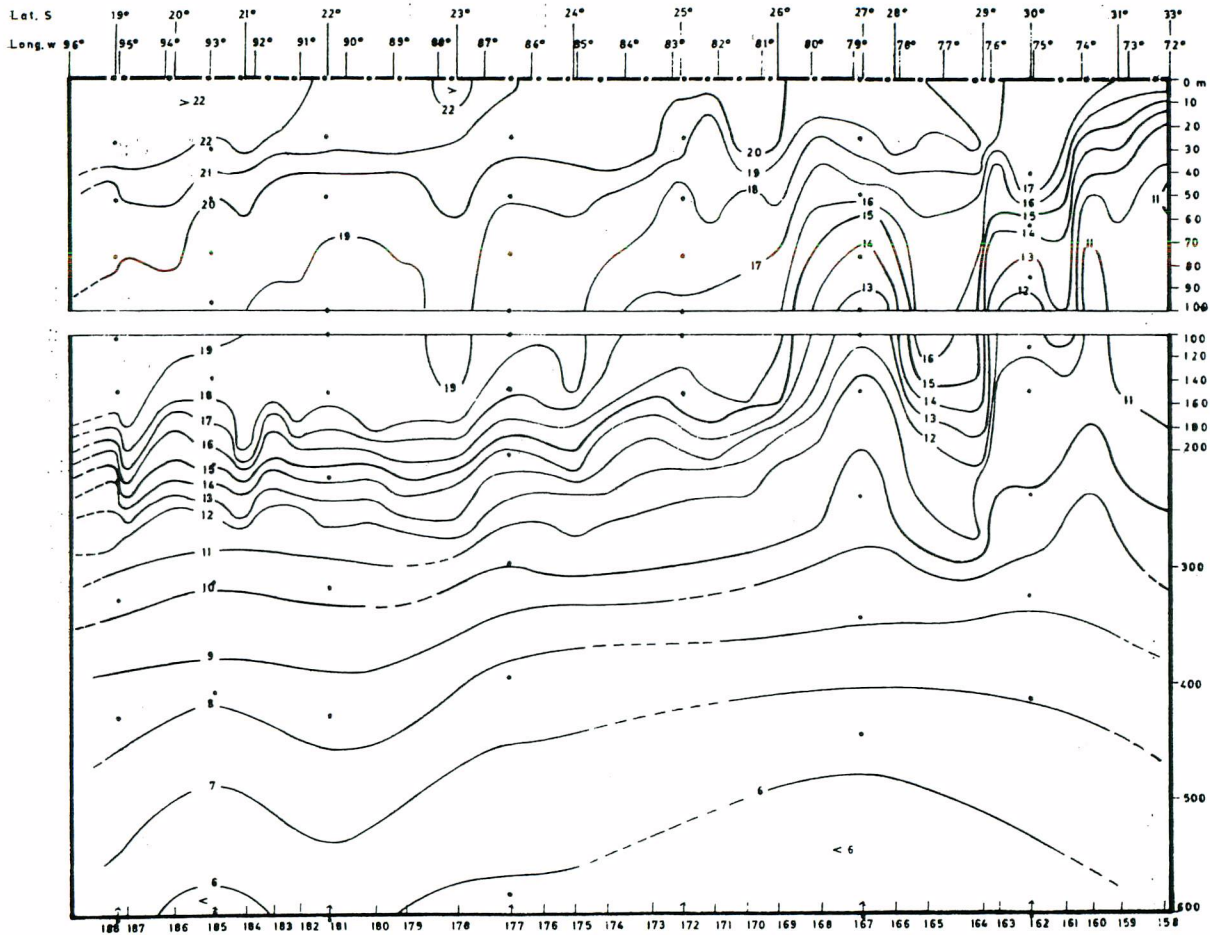


Fig. 17. Salinity profile (%) along section II,



•Oc. St. No.

Fig. 18. Temperature profile (°C) along section III.

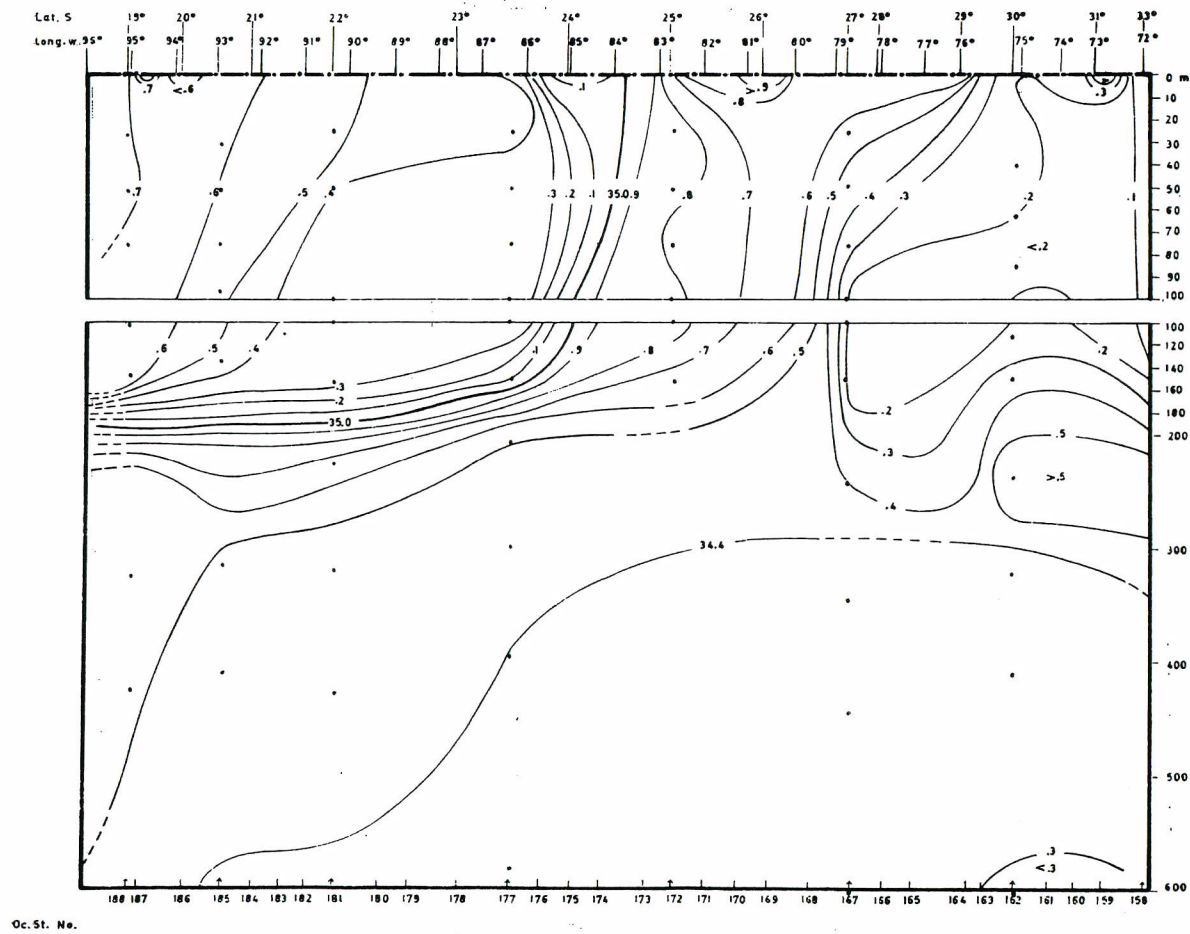


Fig. 19. Salinity profile (%) along section III.

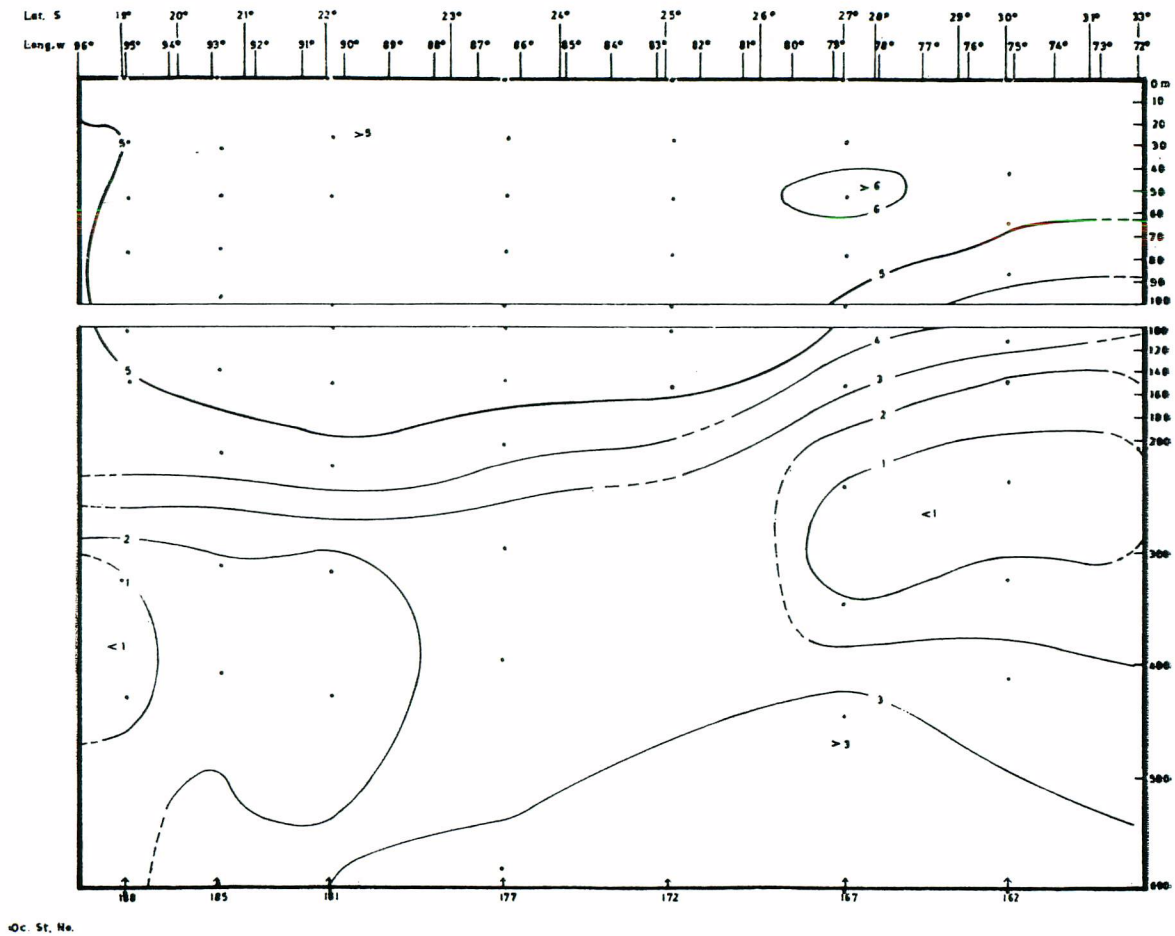


Fig. 20. Oxygen profile (ml/L) along section III.

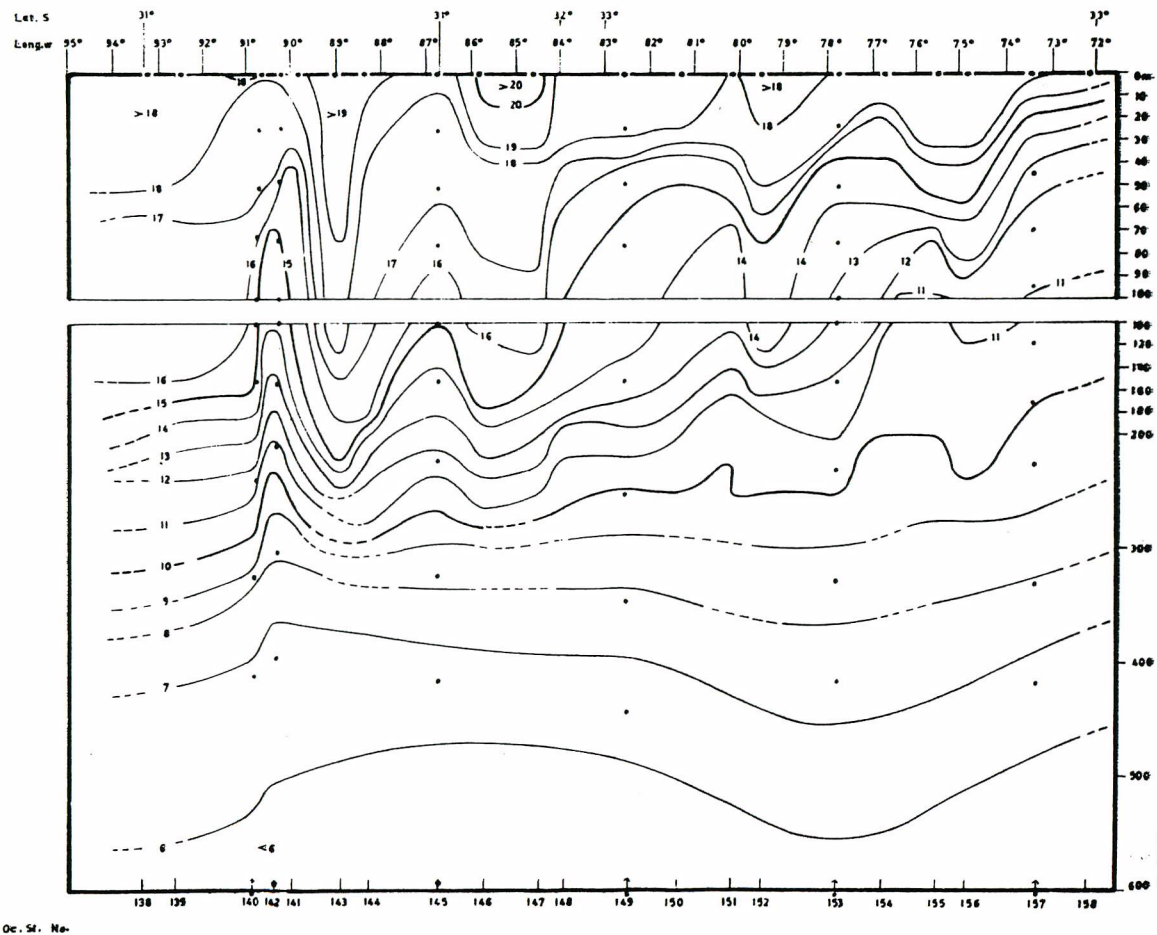


Fig. 21. Temperature profile (°C) along section IV.

The summer distribution of tuna in relation to the general oceanographic conditions off Chile and Peru

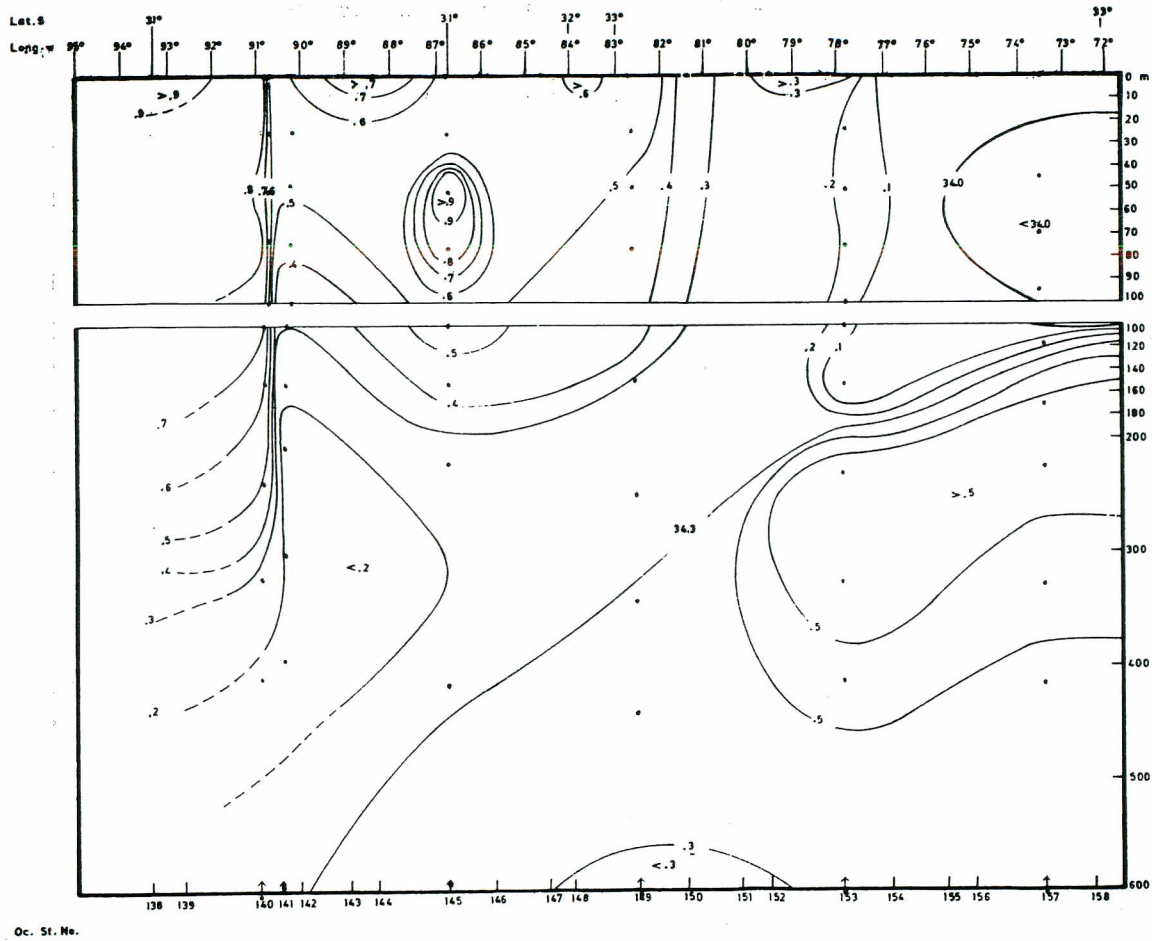


Fig. 22. Salinity profile (%) along section IV.

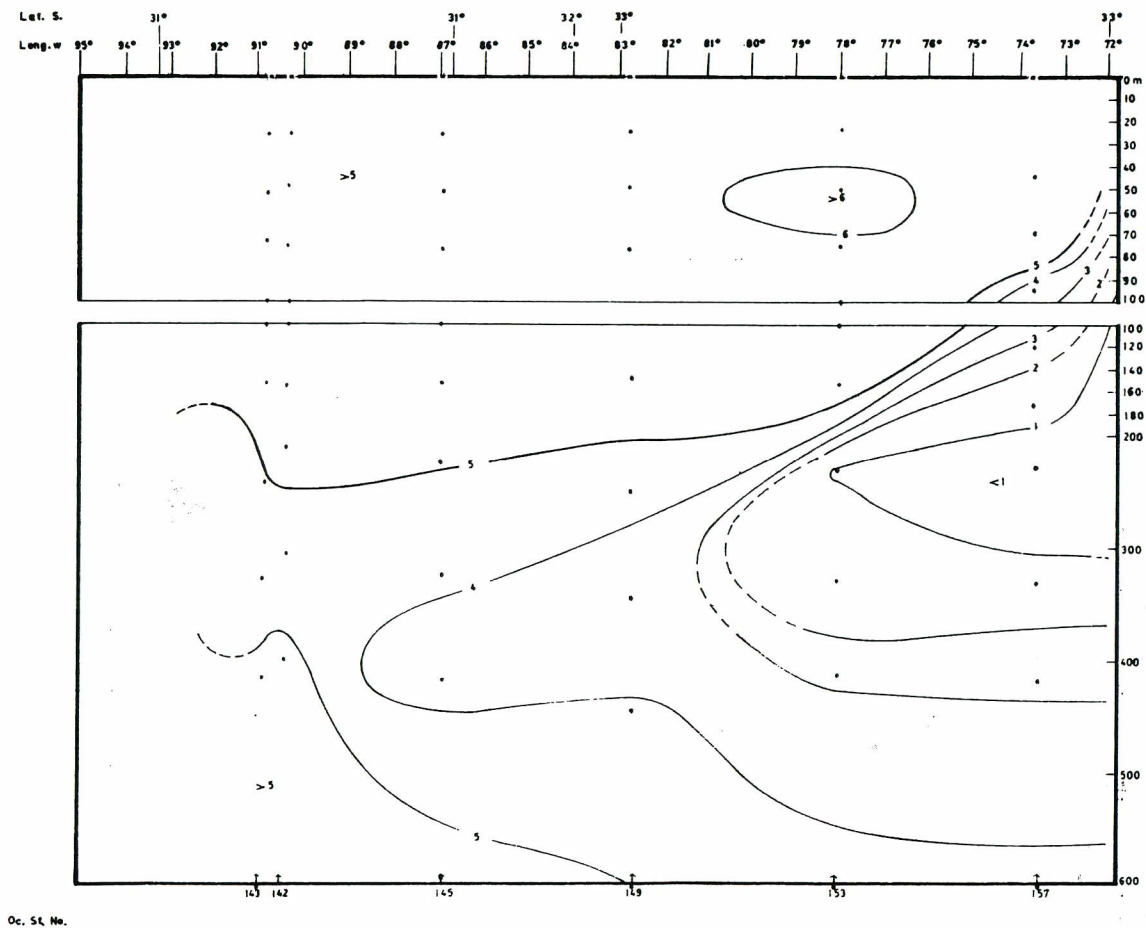


Fig. 23. Oxygen profile (ml/L) along section IV.

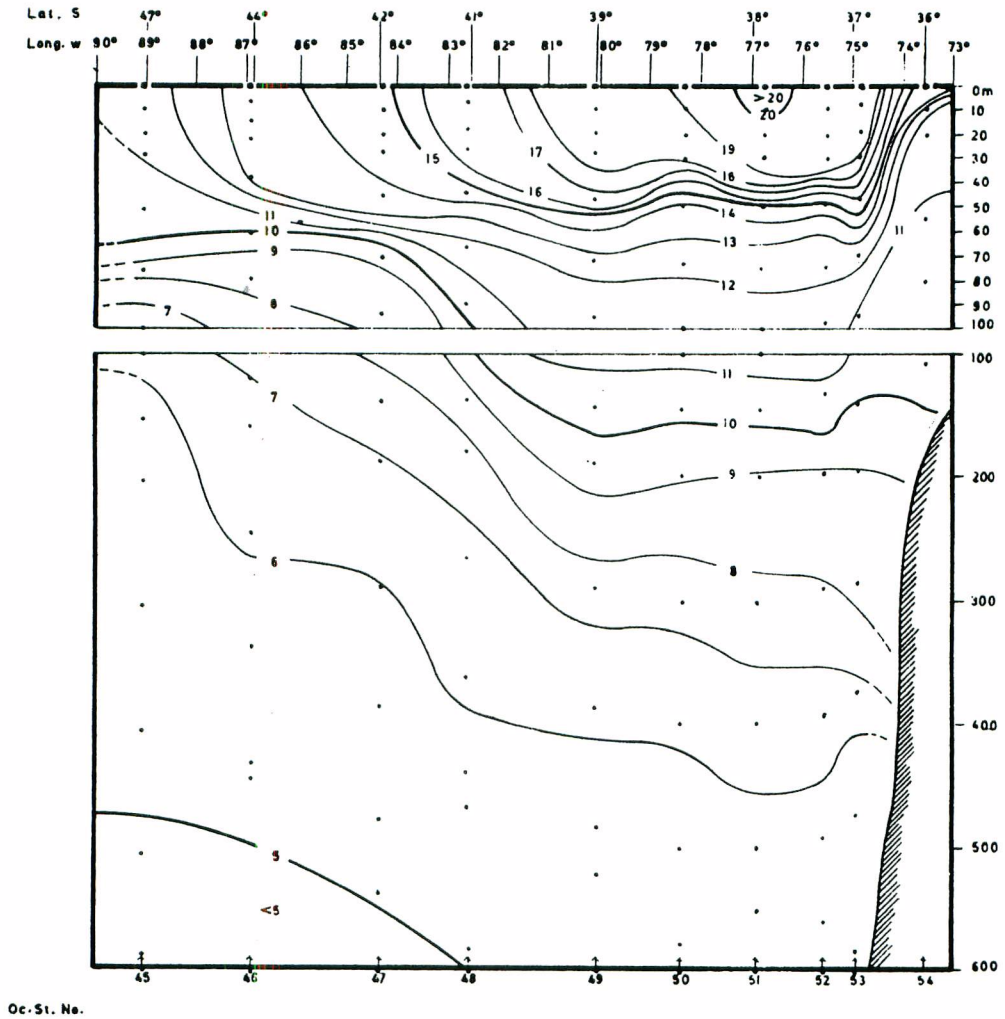


Fig. 24. Temperature profile (°C) along section V

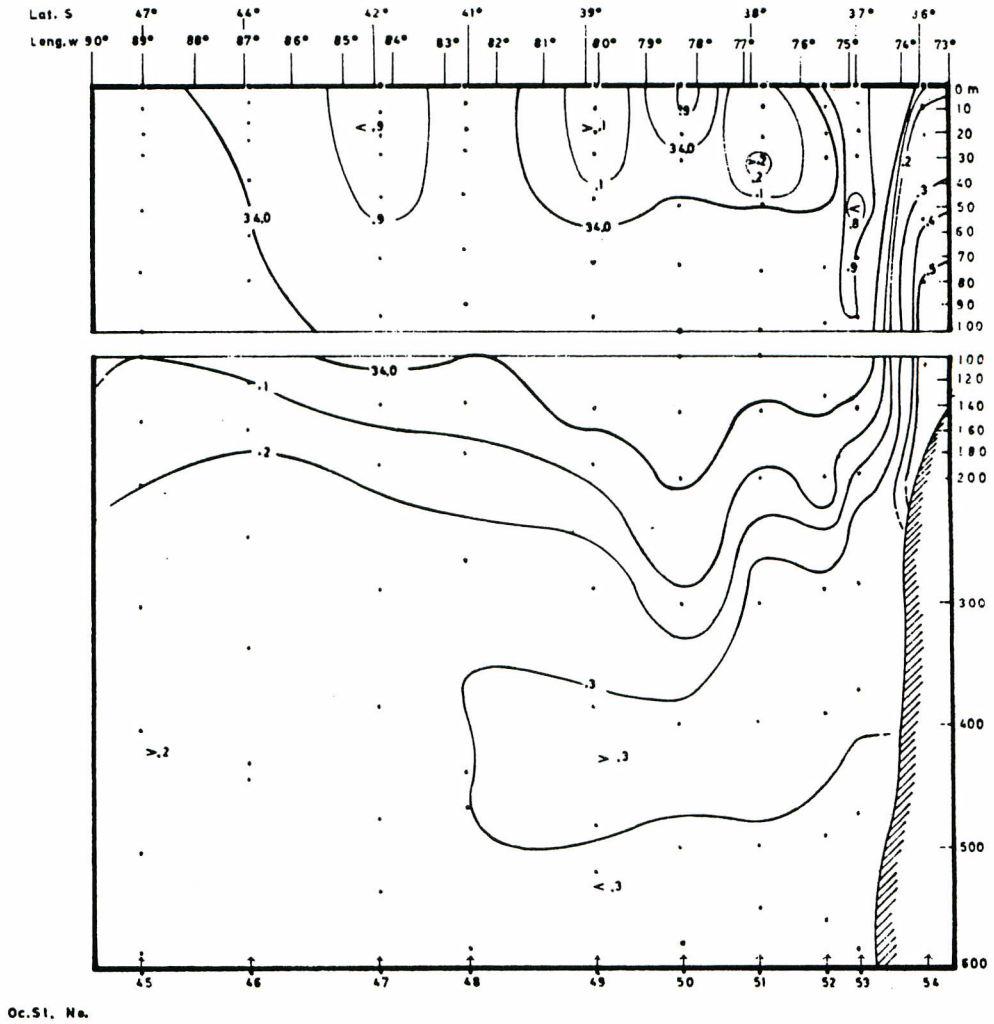
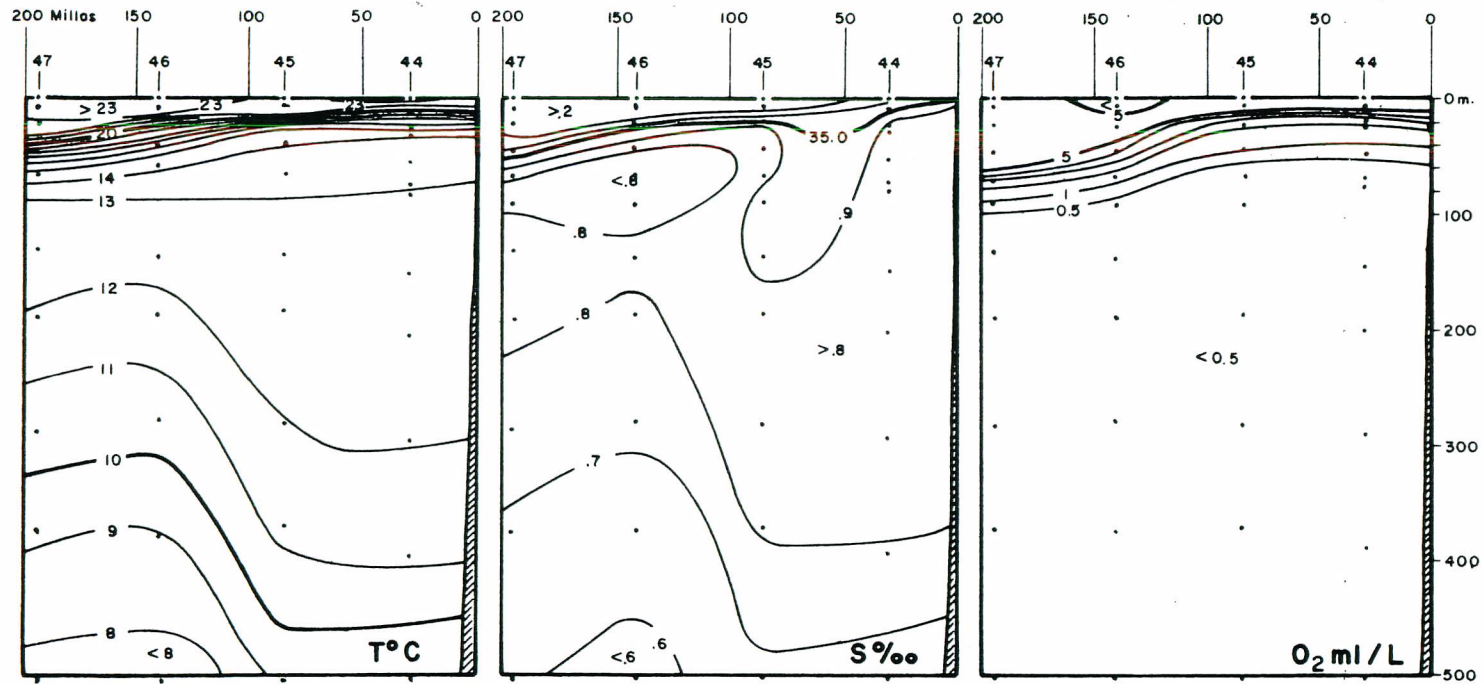
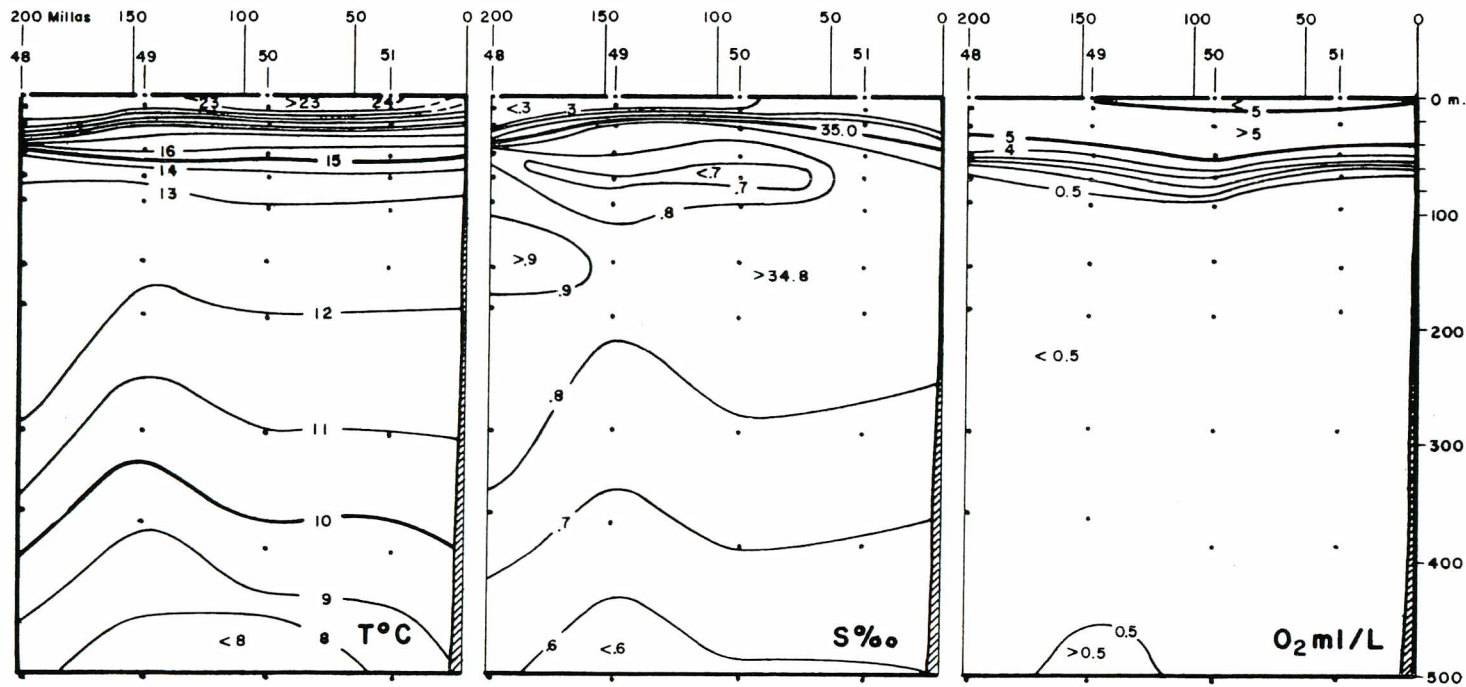


Fig. 25. Salinity profile (%) along section V.



Arica (7-8 Jan. 1969)

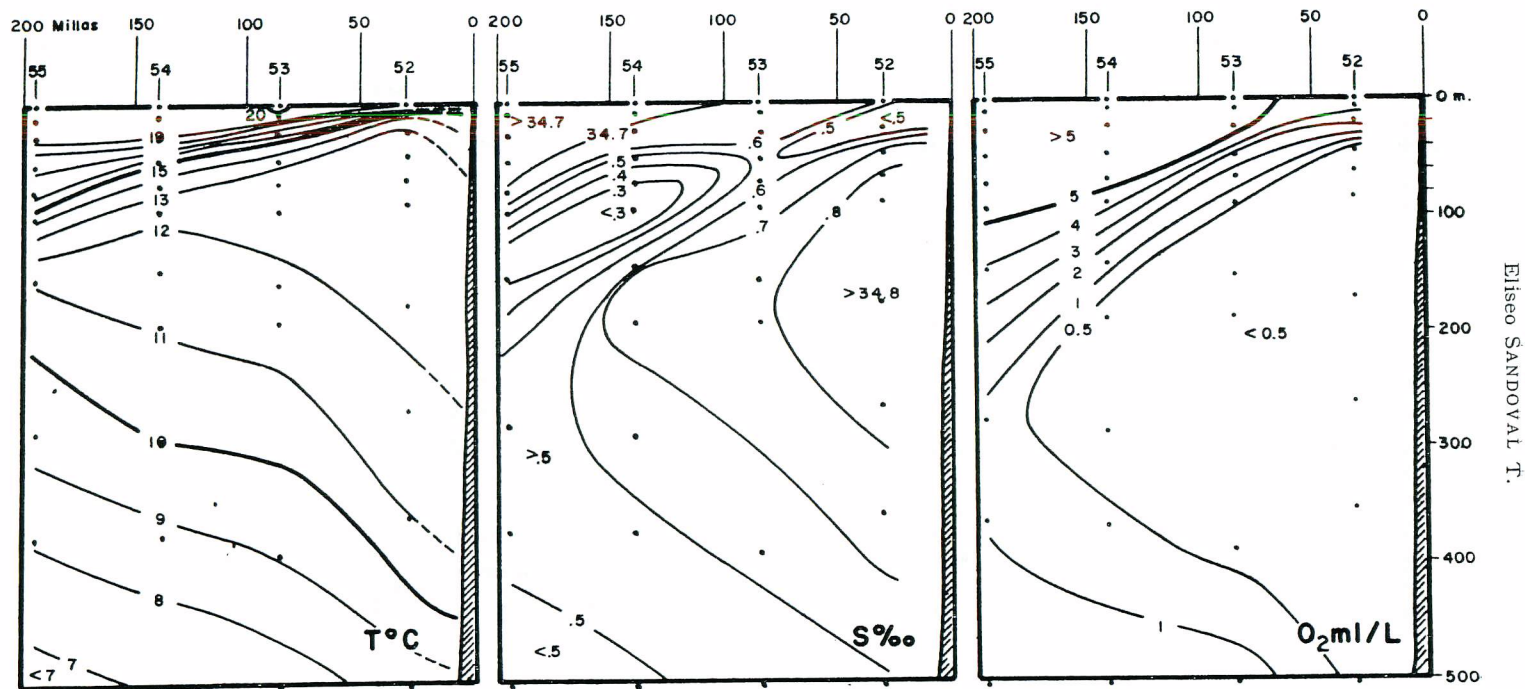
Fig. 26. Profile along section VI-Lat. $18^{\circ}30'S$



Cta. Colorado (8-9 Jan 1969)

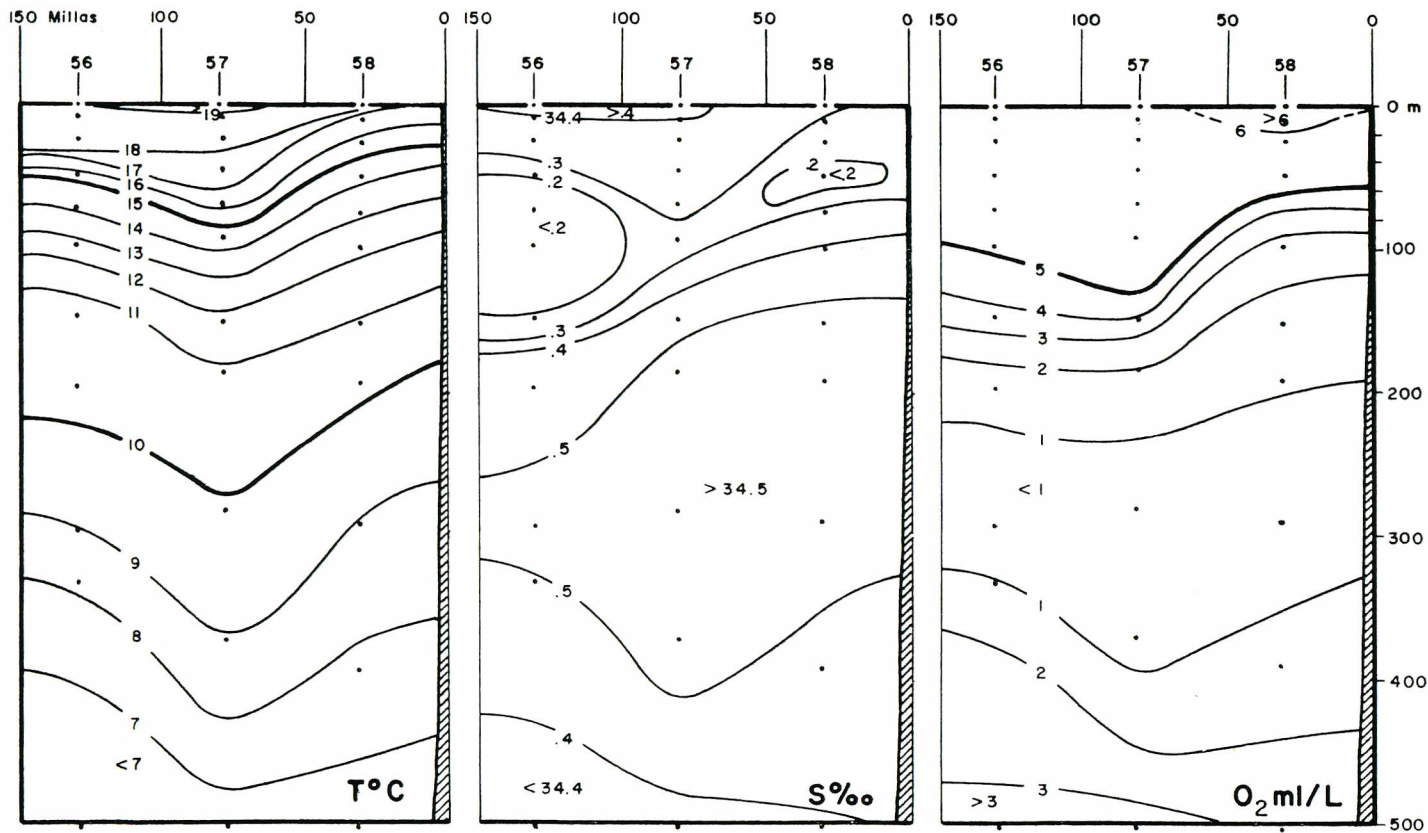
Fig. 27. Profile along section VII-Lat. 20°00'S

The summer distribution of tuna in relation to the general oceanographic conditions off Chile and Peru



Ensa. Paposó (10-11 Jan. 1969)

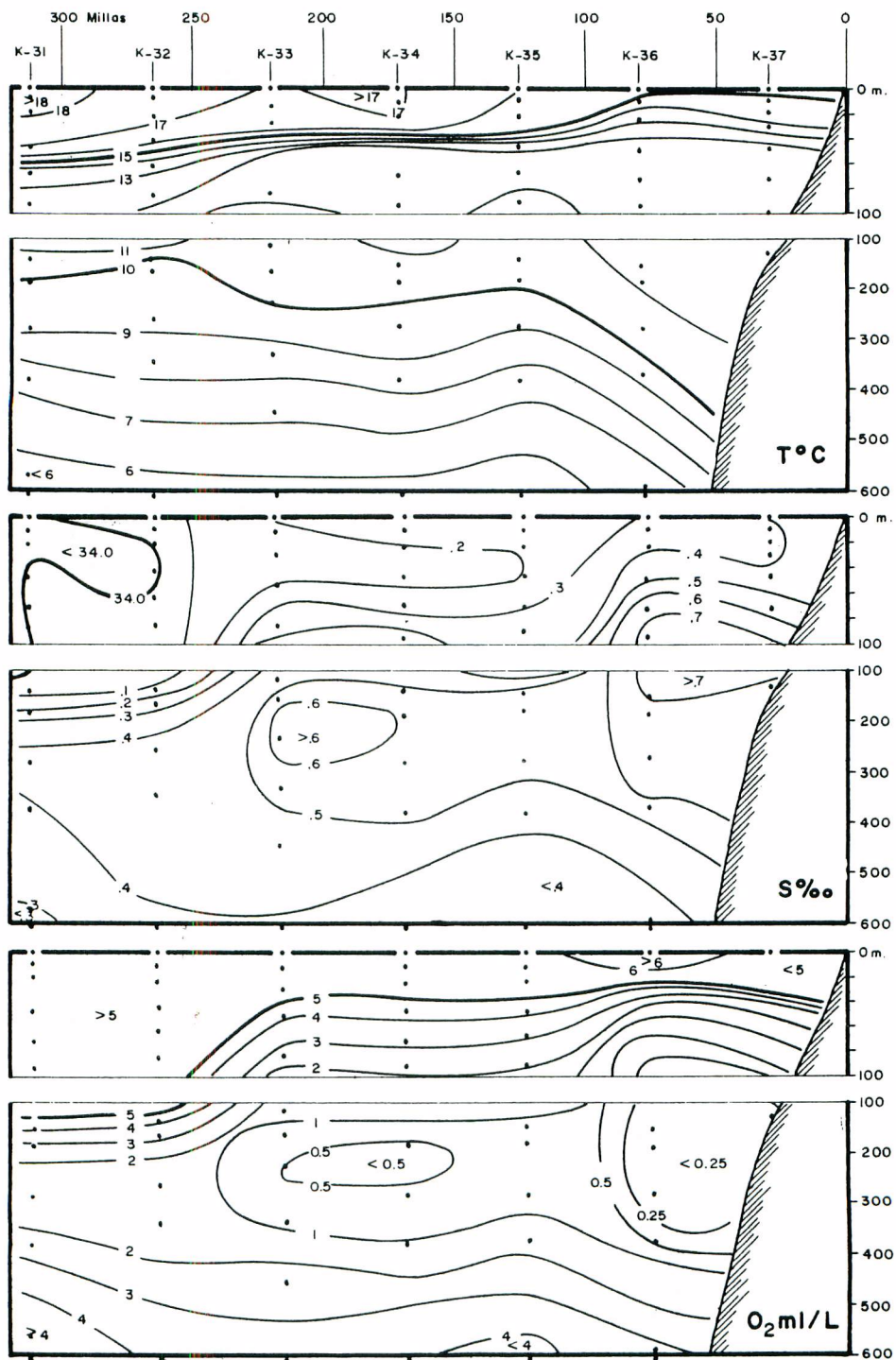
Fig. 28. Profile along section VIII-Lat. 25°00'S



Pto. Coquimbo (12 Jan. 1969)

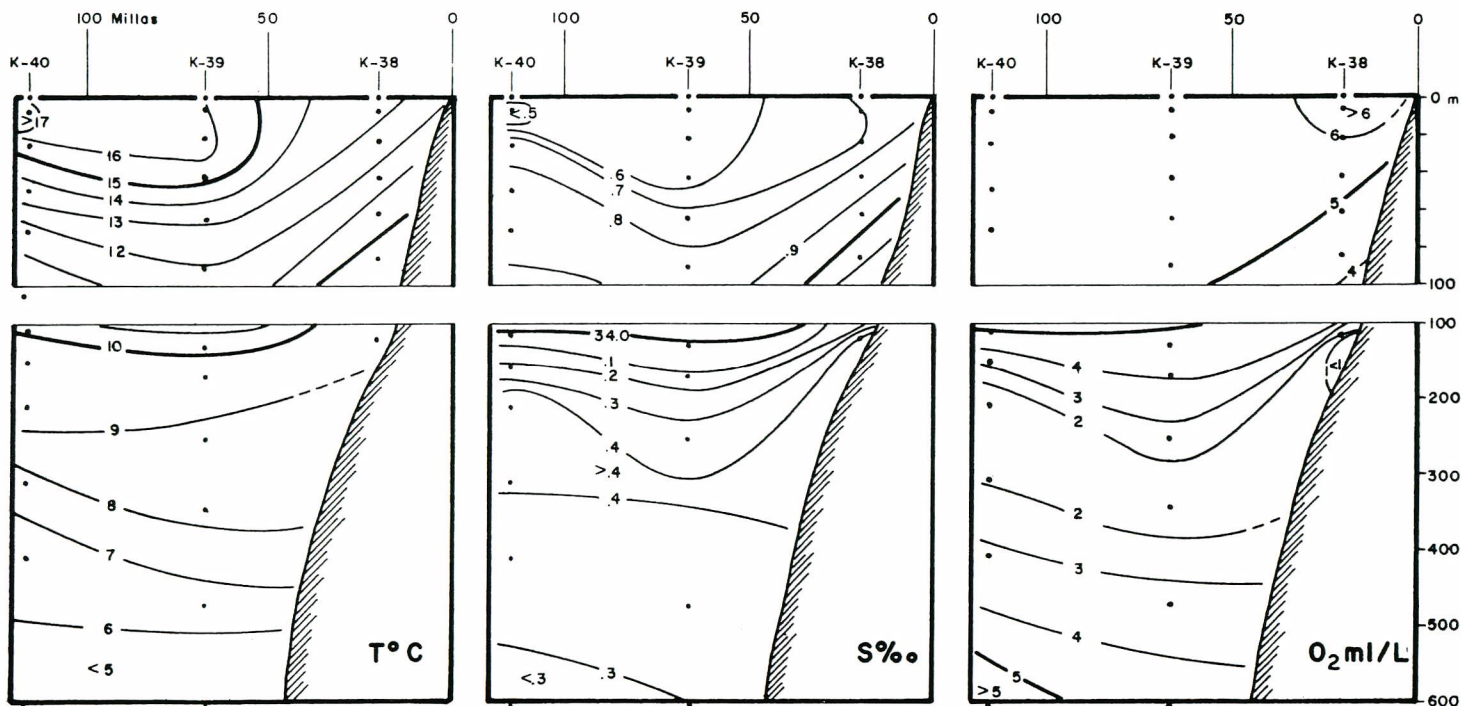
Fig. 29. Profile along section IX-Lat. 30°00'S

The summer distribution of tuna in relation to the general oceanographic conditions of Chile and Peru



Pta. Iloca (12 Feb. 1969)

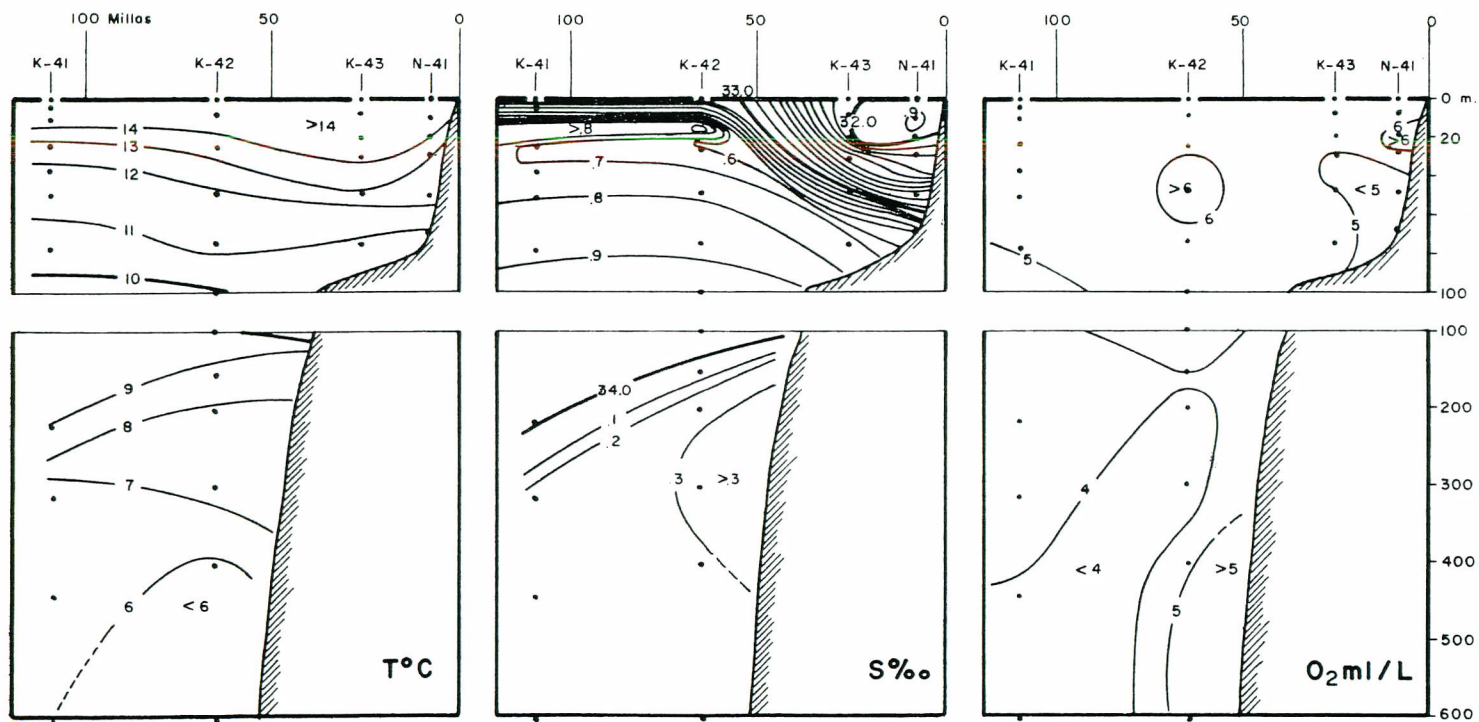
Fig. 30. Profile along section X-Lat. 35°54.3'S



Tta. Galera (30 Jan. 1969)

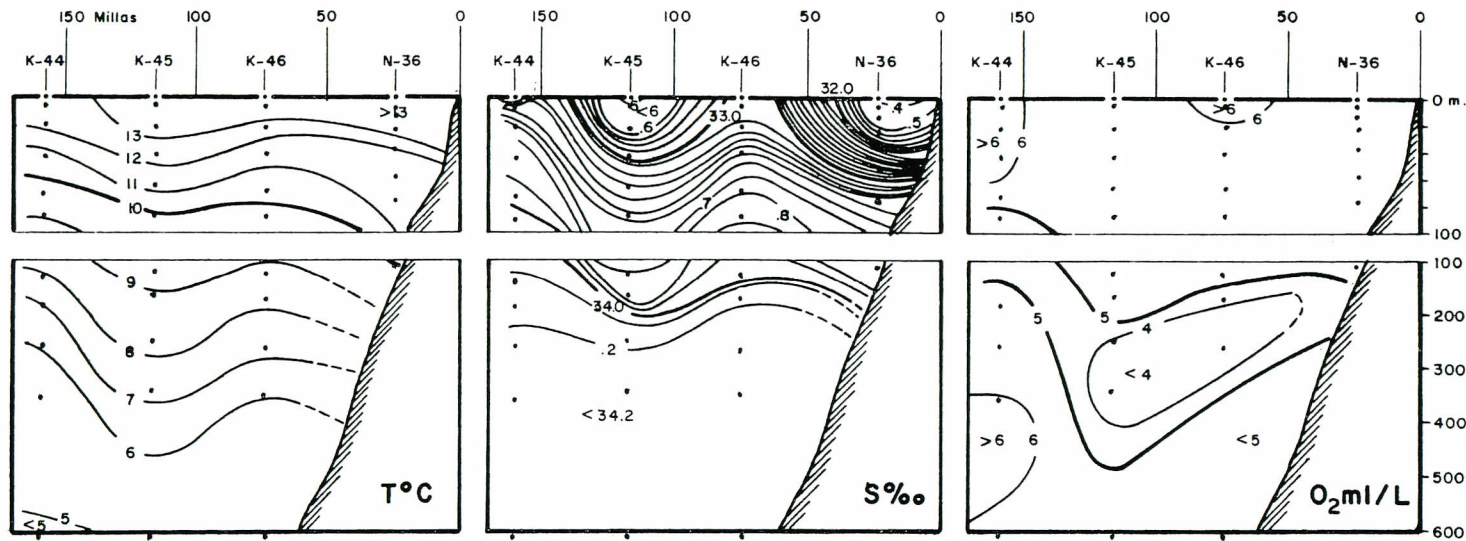
Fig. 31. Profile along section XI-Lat. 40°00'S

The summer distribution of tuna in relation to the general oceanographic conditions off Chile and Peru



Isla Melchor (23-24 Jan. 1969)

Fig. 32. Profile along section XII-Lat. 45°2.5'S.



Golfo de Penas (21-22 Jan. 1969)

Fig. 33. Profile along section XIII-Lat. 47°00'S

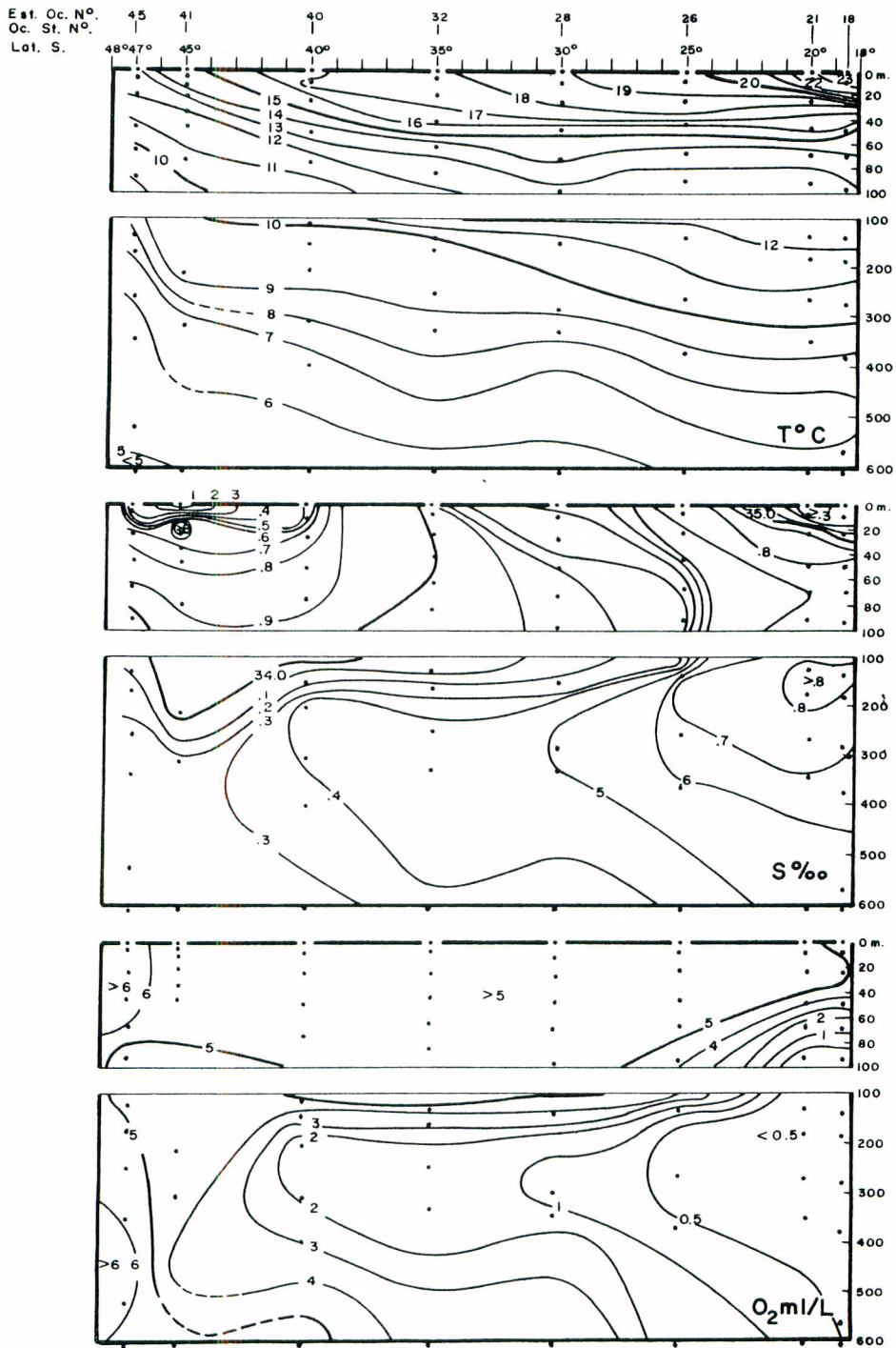


Fig. 34. Longitudinal profile between 120 and 150 miles off the coast. 7 January to 2 February.

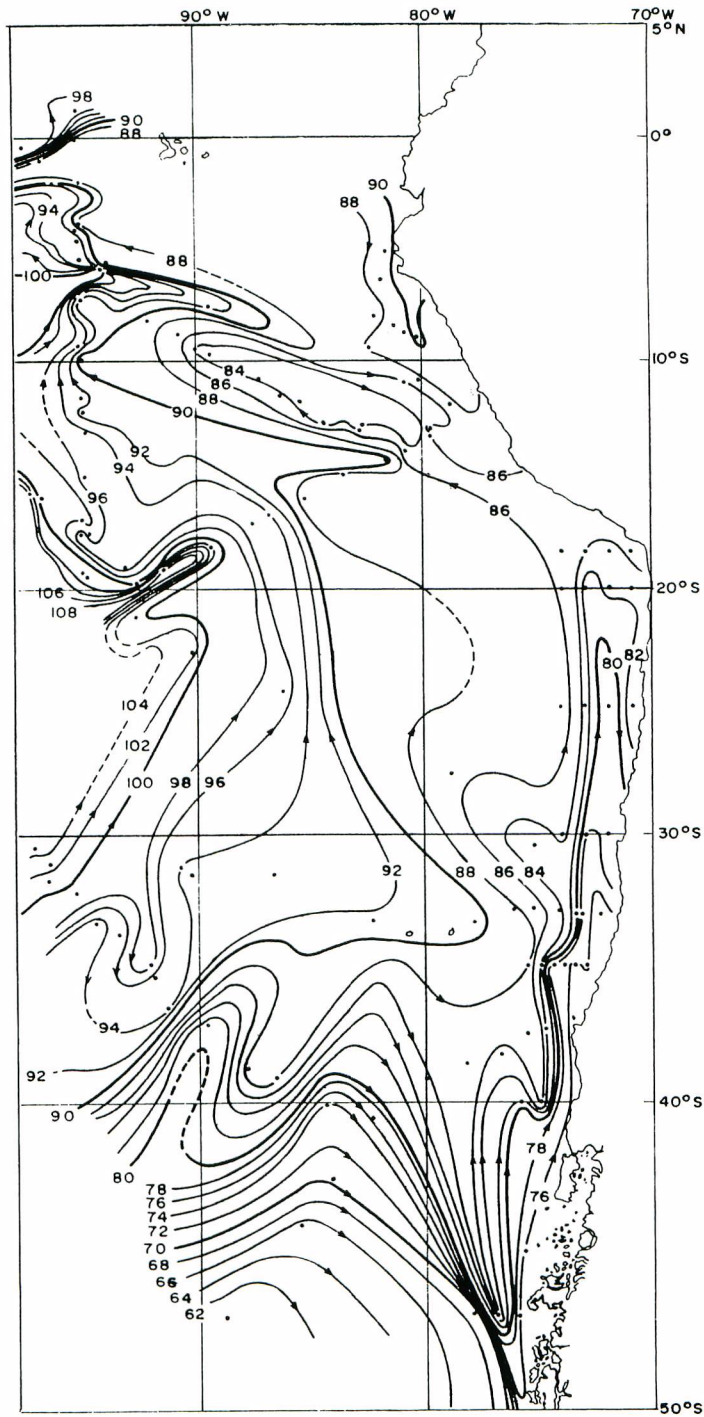


Fig. 35. Geopotential topography at 0 m., relative to 500 decibars.

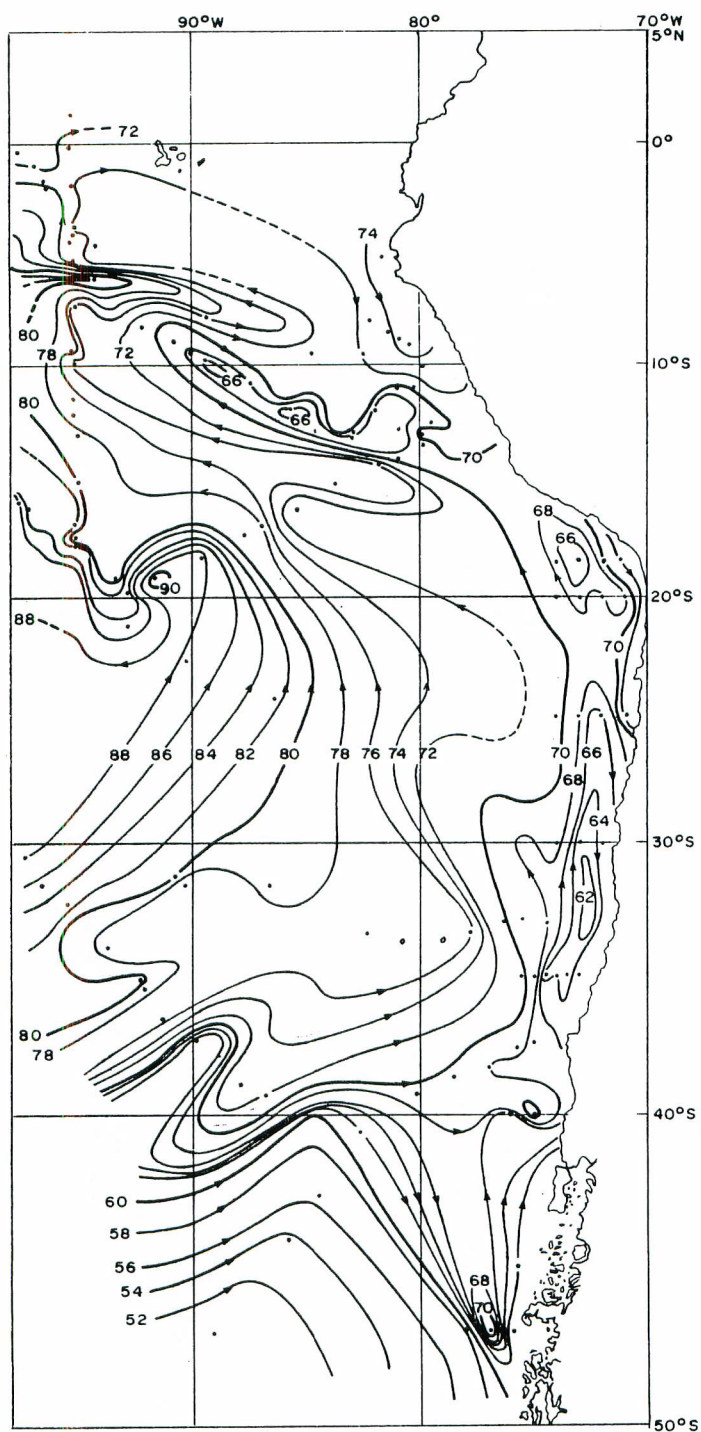


Fig. 36. Geopotential topography at 50 m., relative to 500 decibars

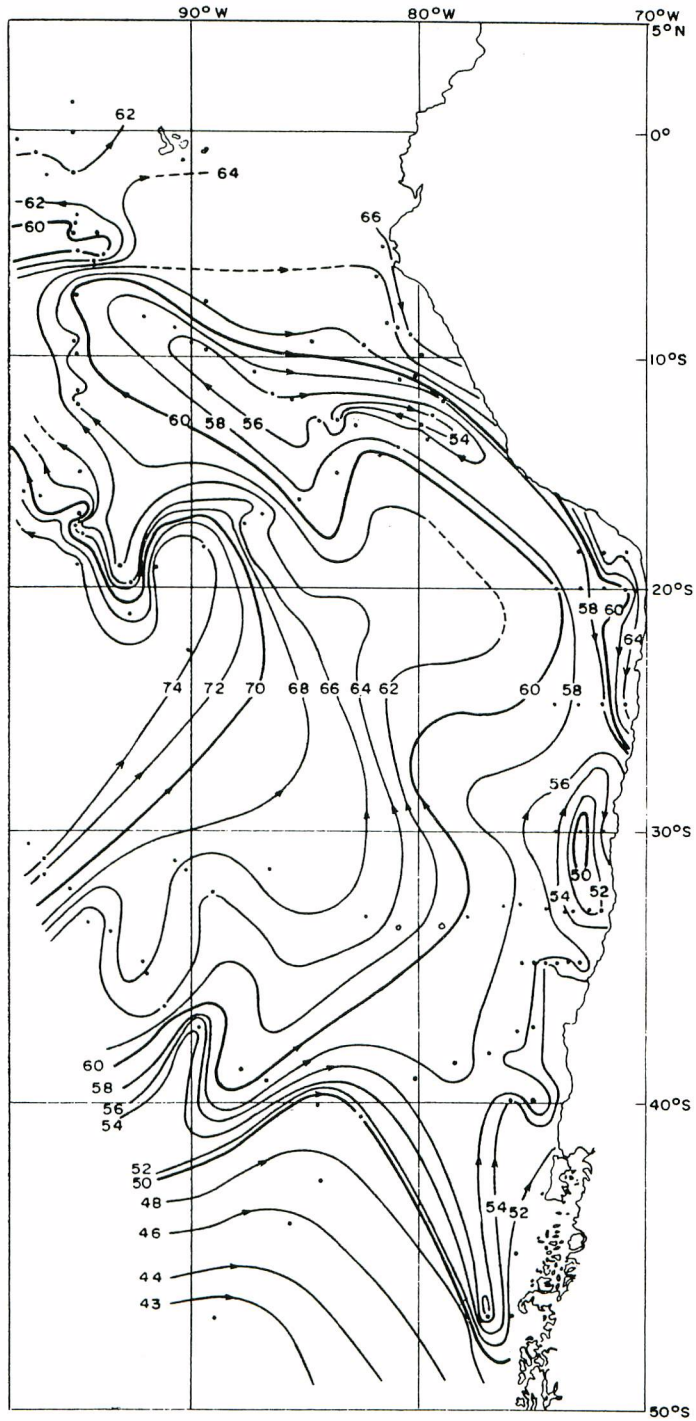


Fig. 37. Geopotential topography at 100 m., relative to 500 decibars.

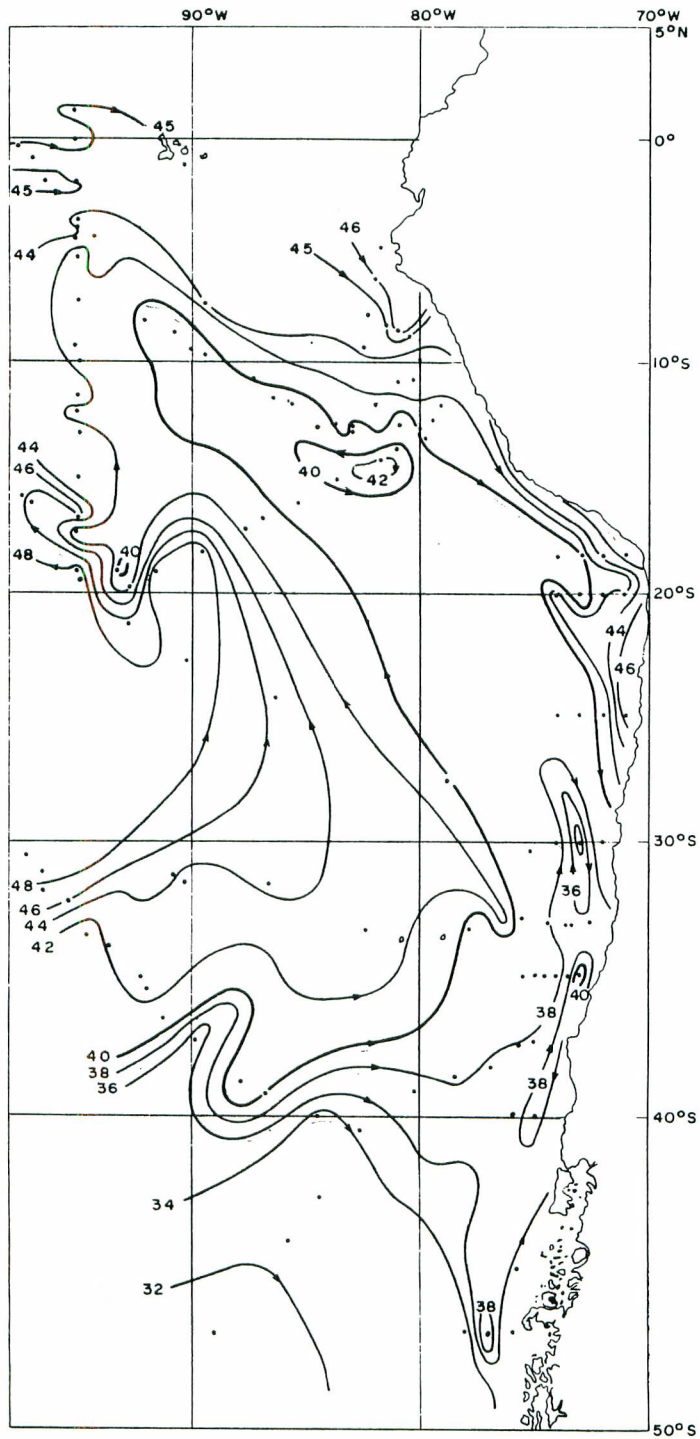


Fig. 38. Geopotential topography at 200 m., relative to 500 decibars.

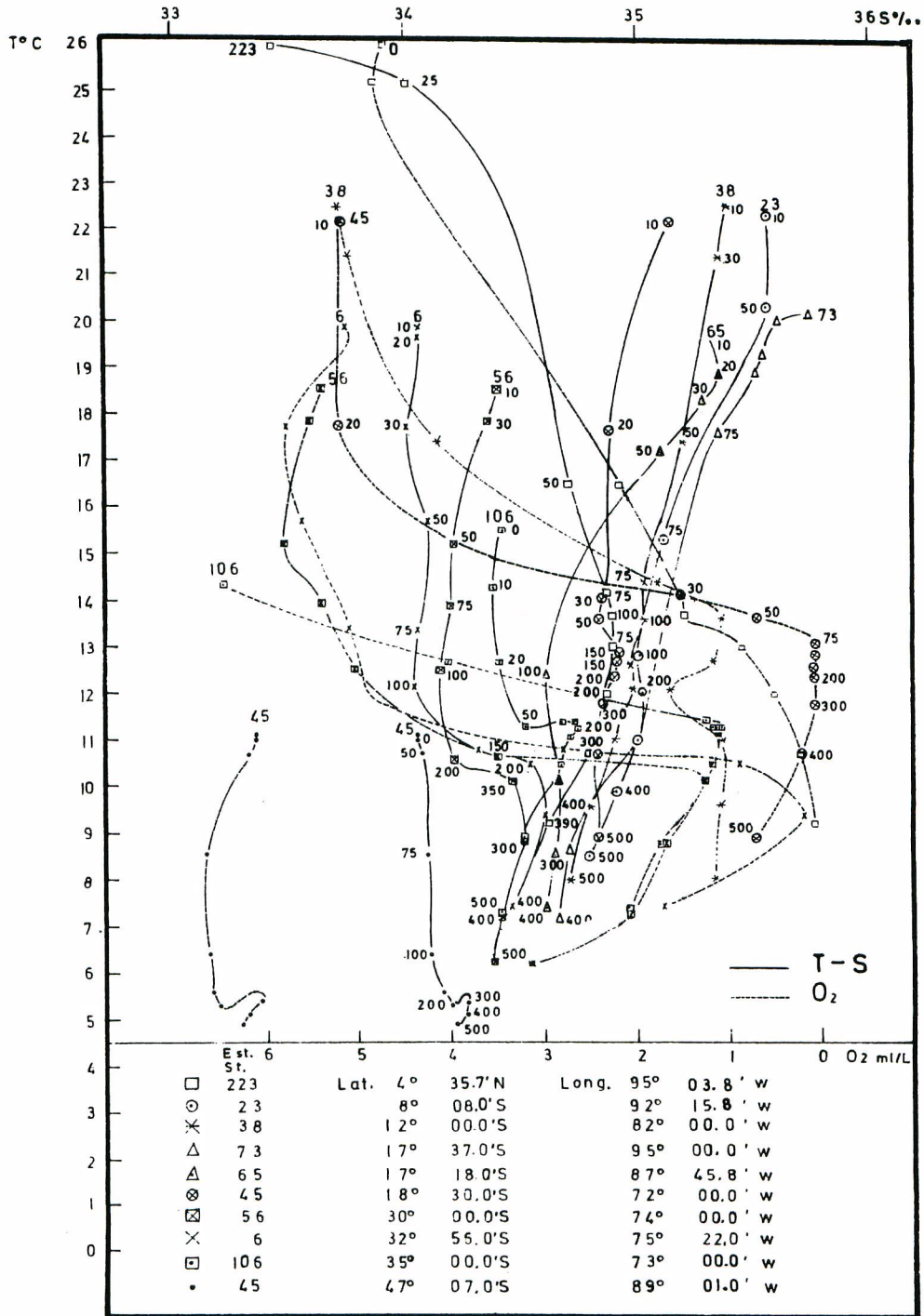


Fig. 39. T-S diagram at ten stations showing the hydrographic structure.

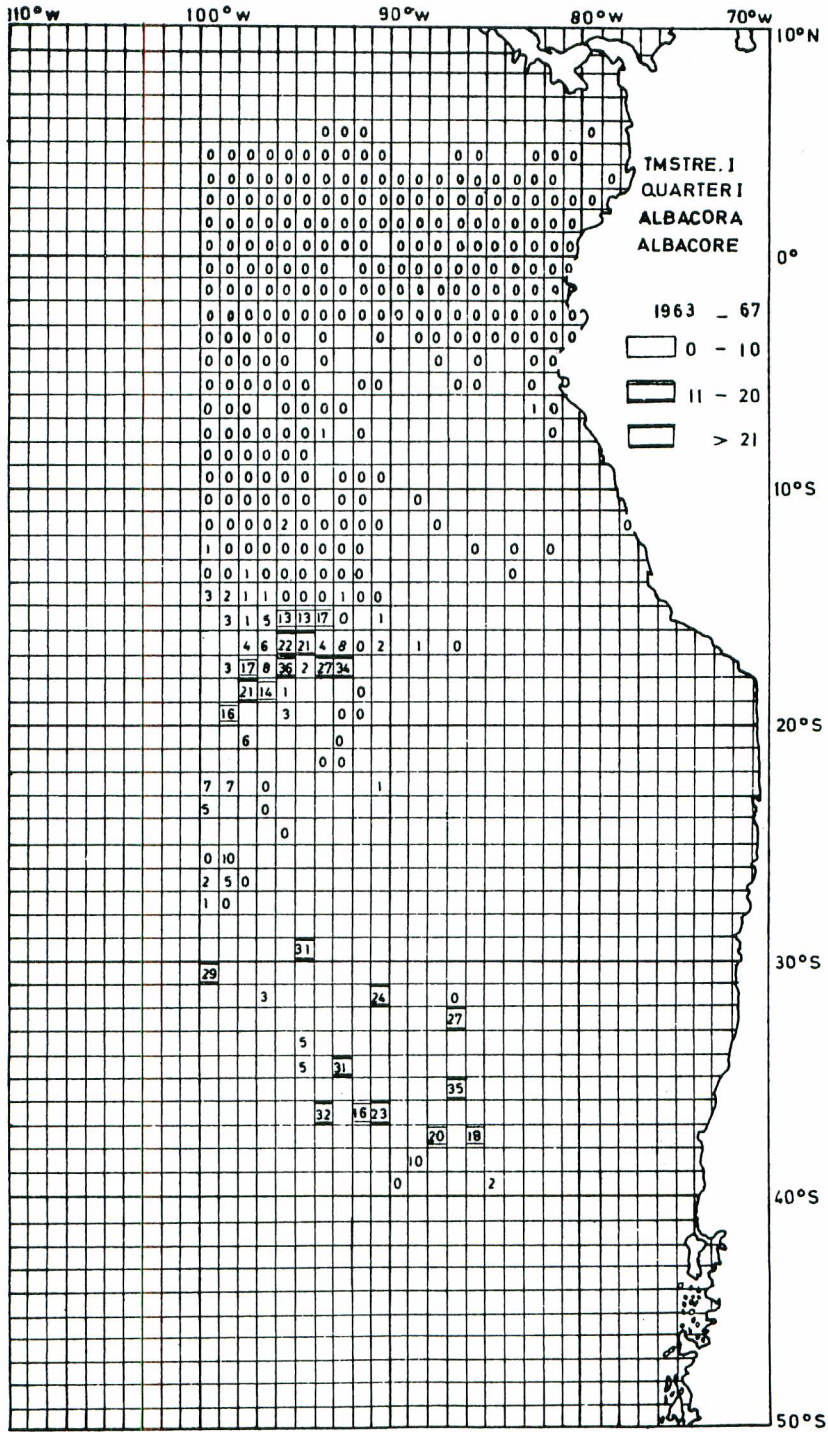


Fig. 40. Average hook rate (catch per 1000 hooks) by 1° areas and by species during 1963-1967.

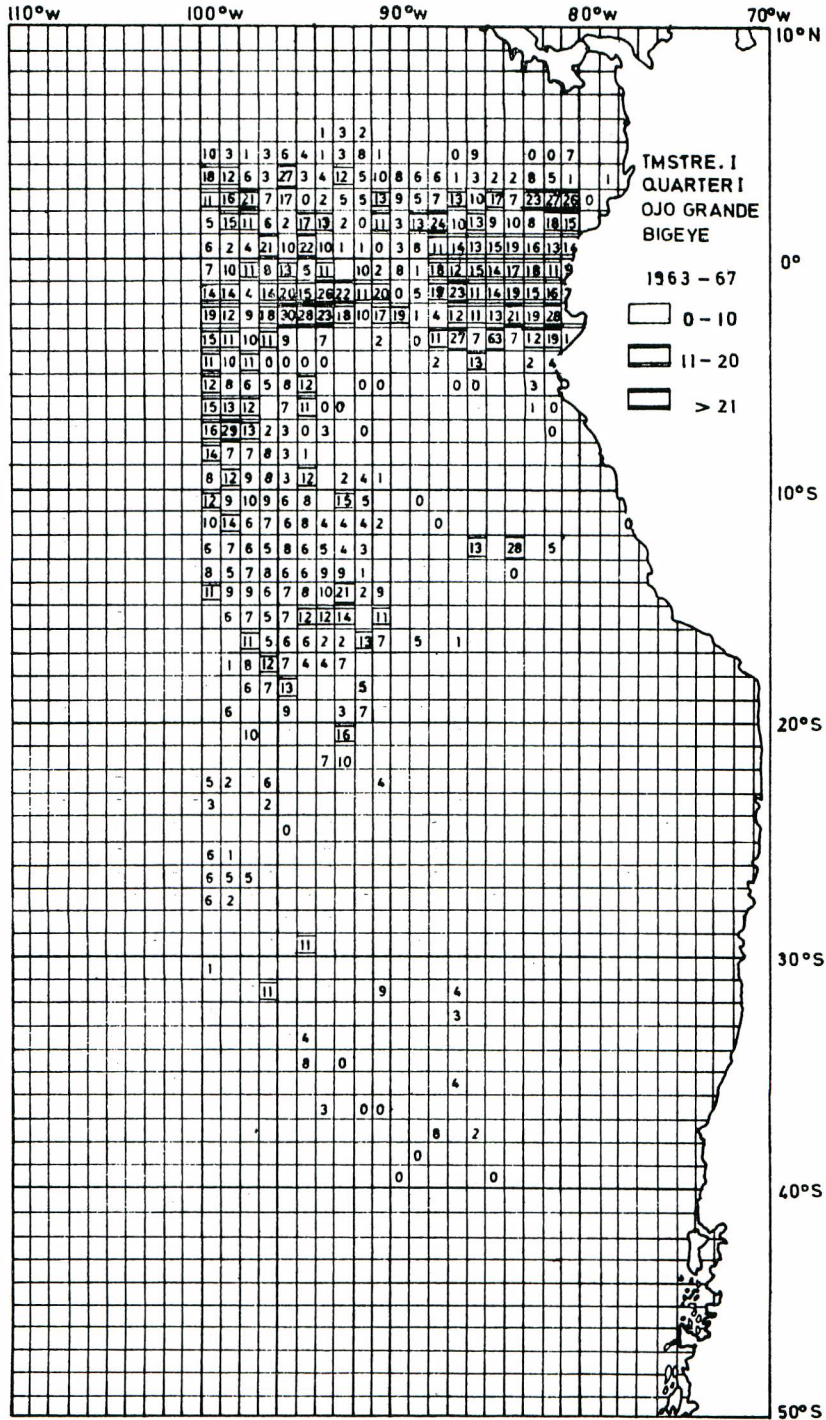


Fig. 41. Average hook rate (catch per 1000 hooks) by 1° areas and by species during 1963-1967.

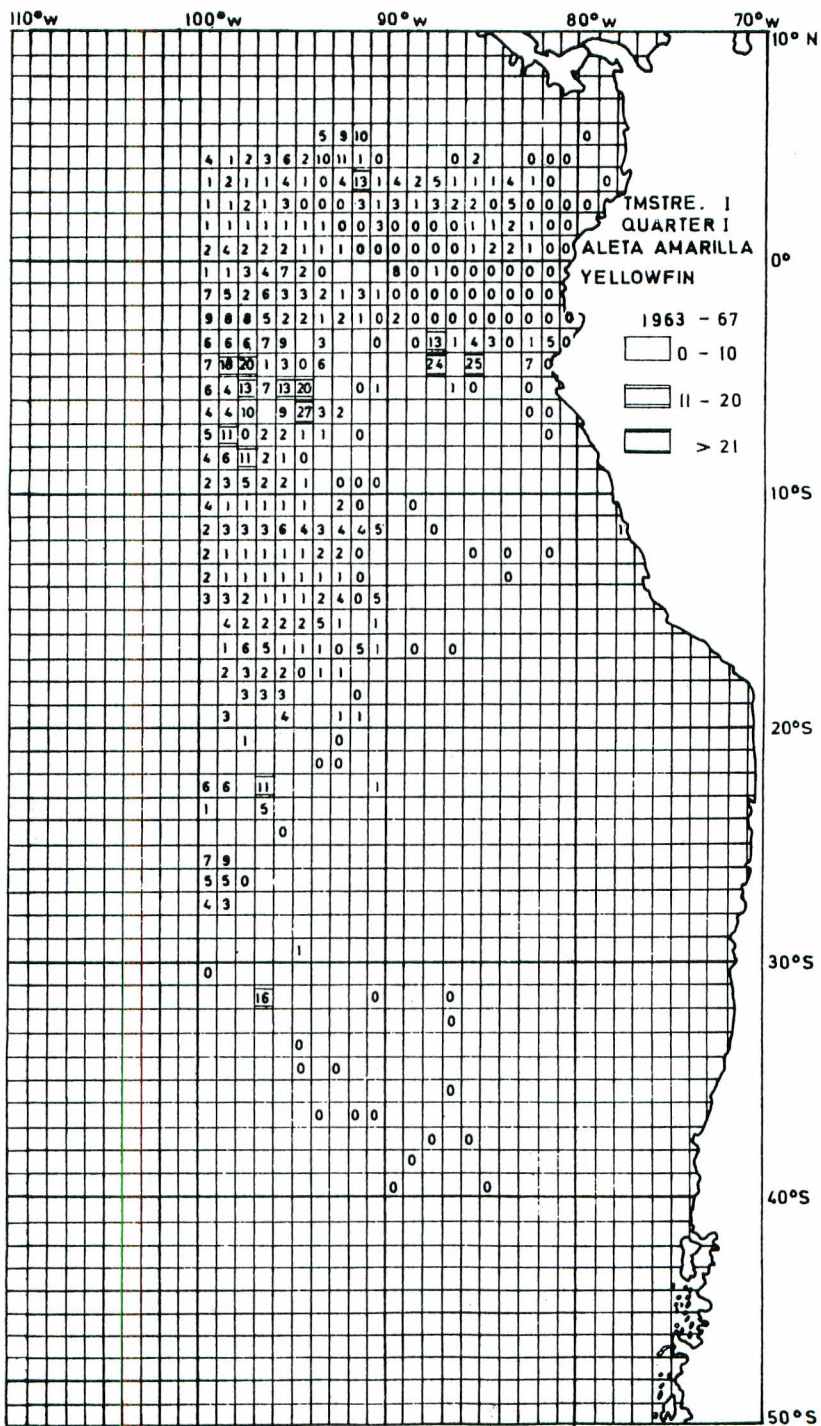


Fig. 42. Average hook rate (catch per 1000 hooks) by 1° areas and by species during 1963-1967.

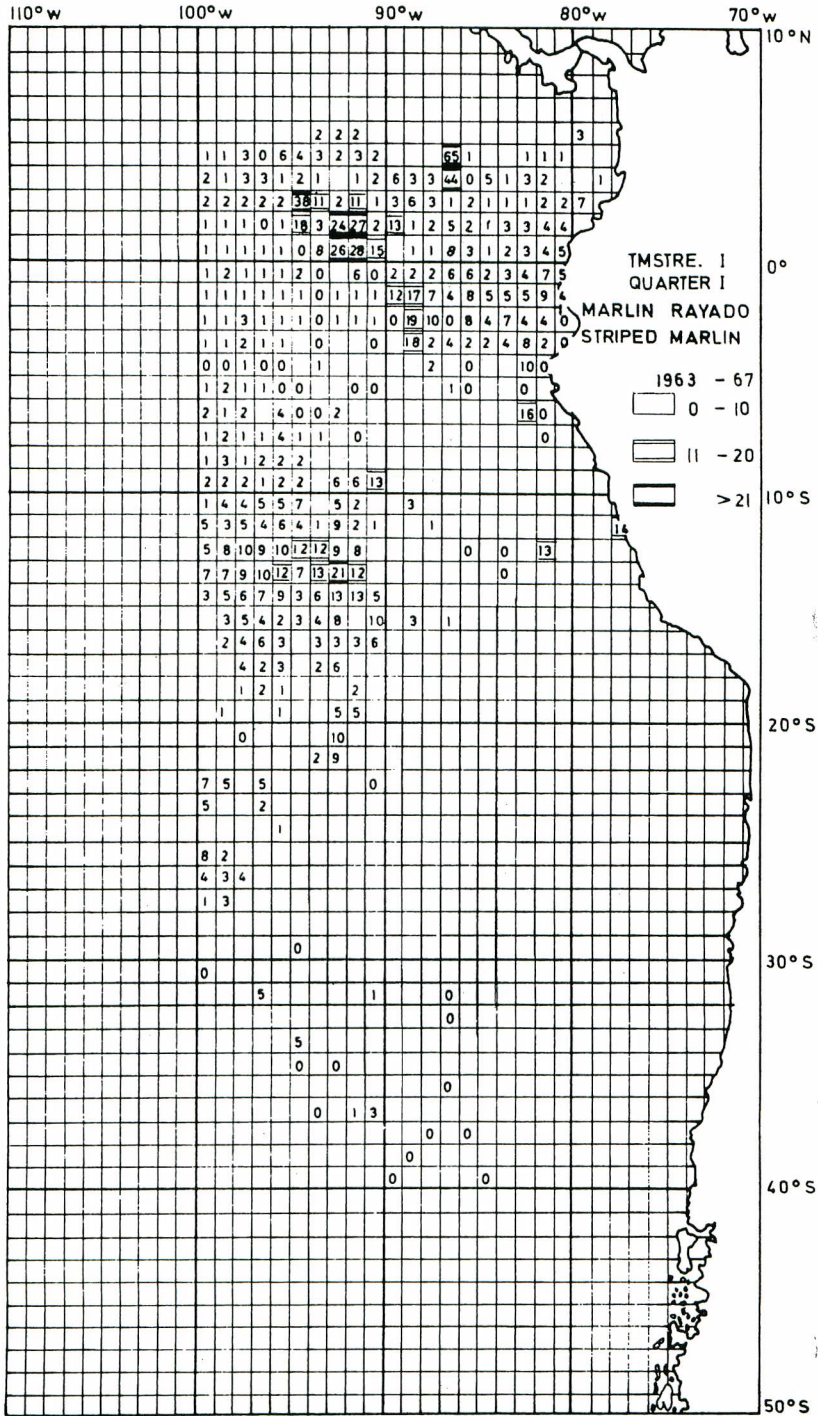


Fig. 43. Average hook rate (catch per 1000 hooks) by 1° areas and by species during 1963-1967.

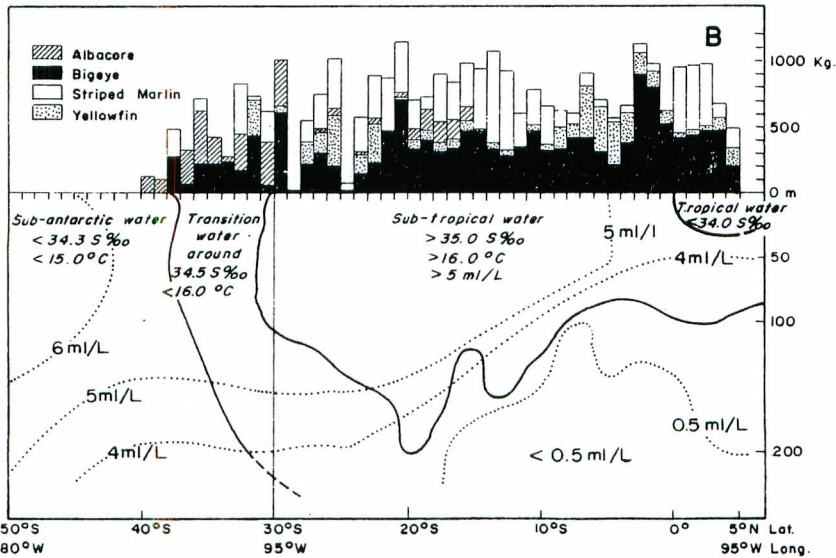
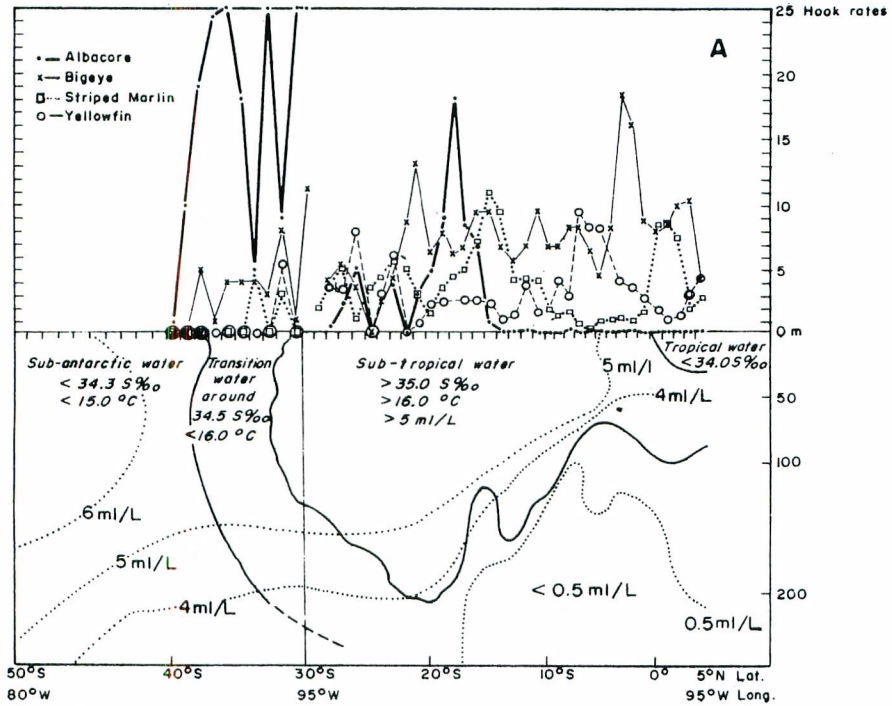


Fig. 44 A. Schematic profile (5°N to 50°S) of the water mass in relation to the average catch per degree of longitude (90° to 100°W) and latitude, in percentage per 1000 hooks.

B. The same, expressed in kilograms.

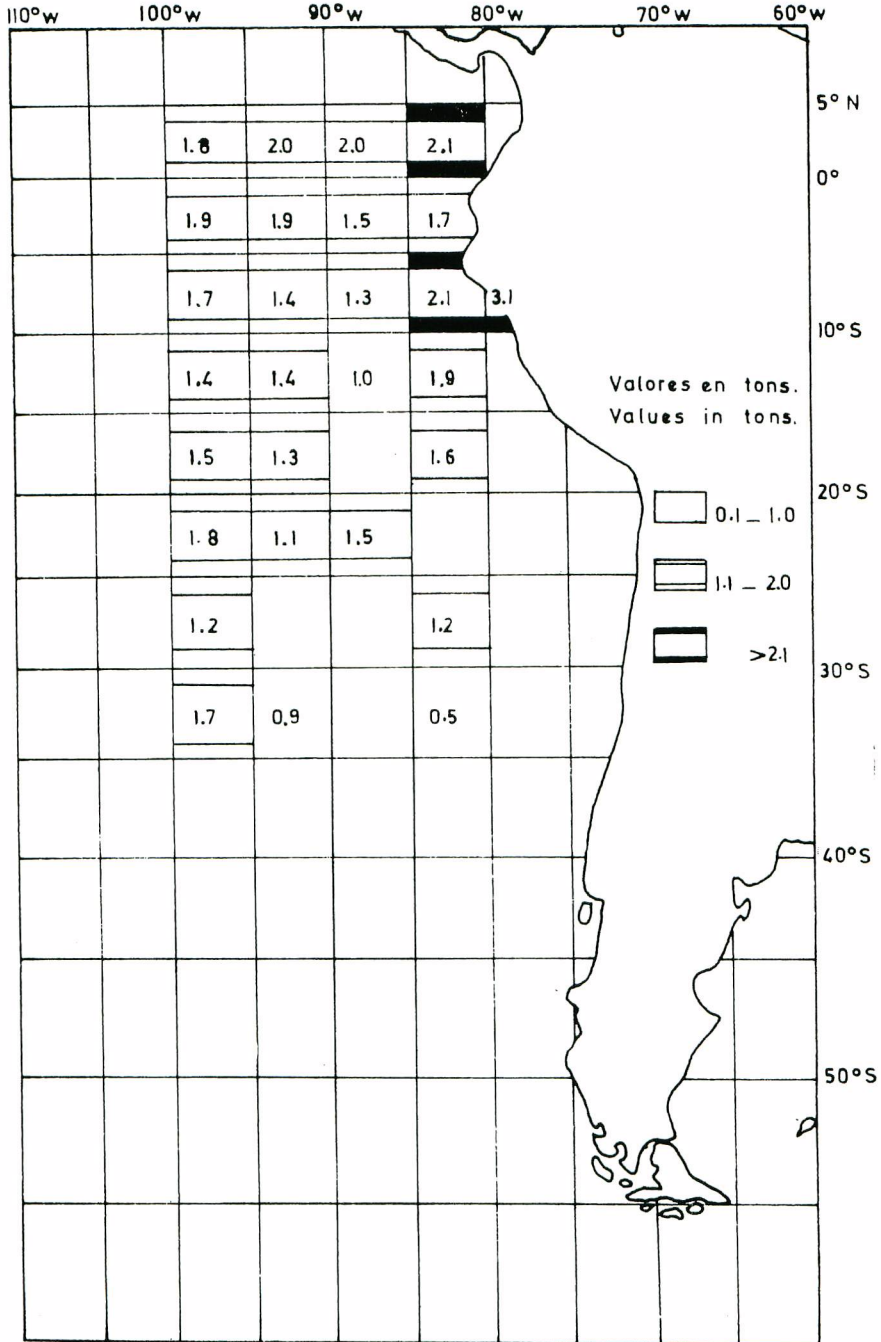


Fig. 45. Average total (catch per 1000 hooks) for all species of tuna and marlin. Dec. 1968-Feb. 1969.

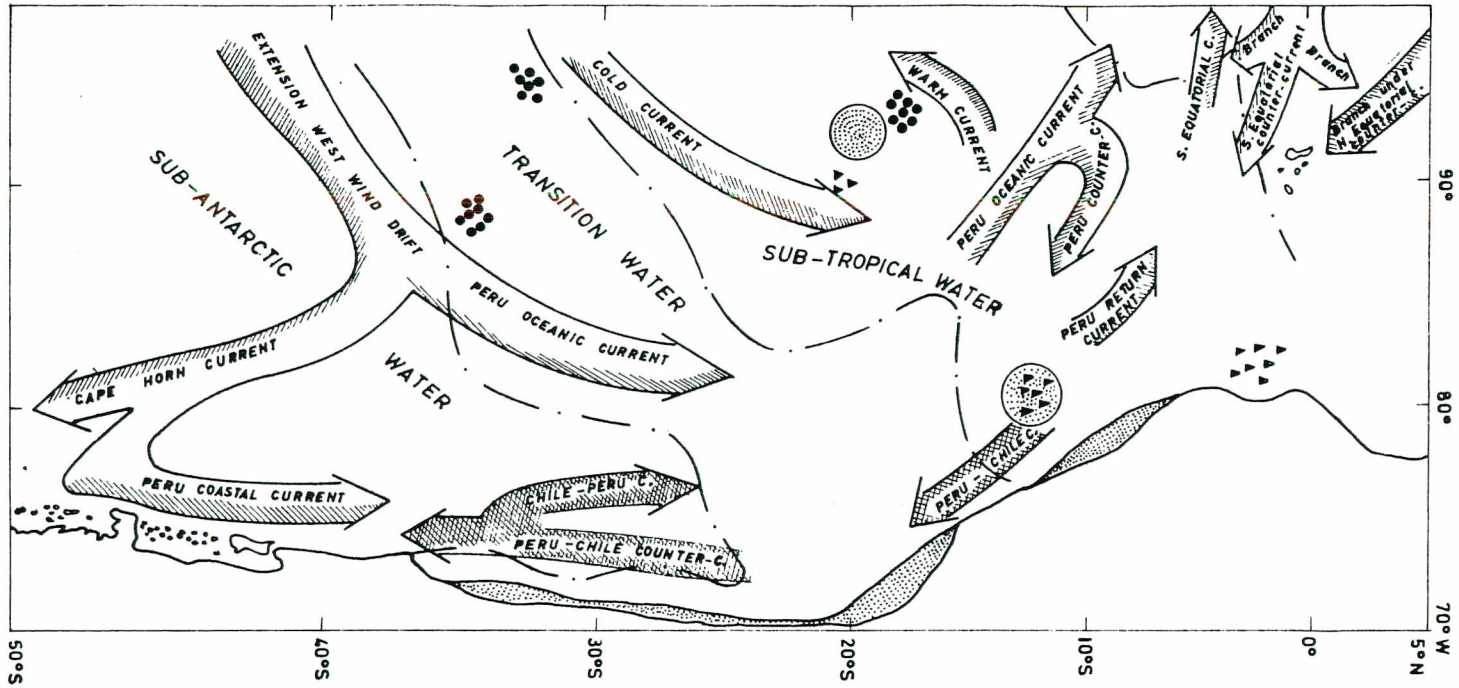


Fig. 46. Schematic Map of Water Masses.

- | | | | |
|-------|--|-------|-----------------------------------|
| — · — | Boundary of water masses at 100 m. depth. | ▲ ▲ ▲ | Good fishing grounds for bigeye |
| → | General drift of the current from 0 m. to 100 m. | • • • | Good fishing grounds for albacore |
| → | General drift of current at 100 m | ⊙ | Upwelling area. |

Table 1. Velocity of current in cm and knots per second in profiles considered.

St. No.	Surface level			Level of 50m		Level of 100 m		Level of 200 m		Level of 300 m	
	★ Miles	# V. c/s	x V. N	V. c/s	V. N.	V. c/s	V. M.	V. c/s	V. N.	V. c/s	V. N.
<i>Profile I</i> Between latitude 5°N and 19°S, longitude 95°W.											
188											
189	31,08	6,25	0,125	6,39	0,128	6,25	0,125	3,07	0,061	1,53	0,031
191	102,12	13,85	0,267	13,27	0,255	13,06	0,250	9,38	0,178	1,14	0,022
192	35,52	7,73	0,155	17,43	0,339	18,74	0,366	18,59	0,362	9,20	0,174
195	108,34	5,40	0,108	4,78	0,096	4,76	0,095	5,66	0,113	5,05	0,101
198	118,10	1,10	0,022	1,74	0,036	3,38	0,067	0,71	0,014	2,83	0,056
199	56,83	8,42	0,168	8,29	0,166	7,05	0,141	3,03	0,061	2,10	0,042
200	39,96	3,49	0,069	2,93	0,059	1,46	0,029	1,46	0,029	1,37	0,027
202	94,71	4,08	0,081	4,28	0,086	3,00	0,060	1,40	0,028	0,74	0,015
203	36,96	24,91	0,488	17,28	0,336	6,05	0,121	0,46	0,009	2,21	0,044
206	121,04	5,33	0,106	6,98	0,139	3,95	0,079	1,35	0,027	1,03	0,021
209	120,12	0,10	0,002	2,71	0,054	2,06	0,041	0,03	0,001	0,10	0,002
210	46,20	1,82	0,036	3,96	0,079	30,43	0,669	24,00	0,470	12,75	0,245
211	31,88	7,02	0,140	8,25	0,165	17,38	0,338	12,64	0,243	13,70	0,264
213	87,78	74,89	1,457	21,74	0,425	14,39	0,278	21,24	0,415	19,43	0,379
214	19,40	339,54	5,841	96,90	1,878	27,04	0,521	42,81	0,836	42,81	0,836
217	110,88	34,59	0,672	4,14	0,083	5,07	0,101	2,59	0,052	3,62	0,072
219	80,85	149,20	2,894	14,78	0,286	18,81	0,366	26,88	0,528	2,55	0,051
<i>Profile II</i> Between latitude 12°S and 19°S, longitude 78° and 93°W.											
69											
67	129,65	2,33	0,046	1,69	0,034	0,72	0,014	0,29	0,006	0,23	0,005
65	125,65	10,28	0,195	9,79	0,186	8,87	0,177	7,00	0,140	2,74	0,055
64	48,84	0,59	0,012	0,75	0,015	0,71	0,014	0,53	0,010	3,47	0,069
62	97,68	10,52	0,200	10,00	0,190	8,77	0,175	0,56	0,011	1,40	0,028
59	117,66	0,92	0,018	0,54	0,011	0,51	0,010	1,04	0,021	0,75	0,015
56	122,10	4,63	0,093	3,42	0,061	2,88	0,058	1,60	0,032	0,84	0,017
52	128,32	7,01	0,140	6,29	0,126	4,58	0,092	2,22	0,044	1,35	0,027
<i>Profile III</i> Between latitude 33° to 19°S, longitude 72° and 95°W.											
188											
185	145,20	2,35	0,047	2,02	0,040	1,74	0,035	1,20	0,024	0,78	0,016
181	159,60	1,41	0,028	1,47	0,029	1,56	0,031	1,48	0,029	1,25	0,025
177	219,20	2,23	0,045	1,93	0,039	1,80	0,036	1,47	0,029	0,93	0,019
167	440,80	1,56	0,031	1,65	0,037	1,49	0,026	0,72	0,014	0,24	0,025
162	170,00	138,14	2,683	126,74	2,465	121,67	2,363	55,34	1,077	12,25	0,235
<i>Profile IV</i> Between latitude 33° to 31°S, longitude 72° and 95°W.											
142											
145	191,20	0,81	0,016	0,82	0,016	0,87	0,017	0,70	0,014	0,25	0,005
149	248,00	40,25	0,825	44,77	0,865	38,23	0,745	45,17	0,873	25,48	0,499
153	236,00	21,87	0,427	33,68	0,654	130,68	2,544	87,50	1,700	29,07	0,561
157	235,20	39,42	0,768	34,80	0,676	20,80	0,406	6,87	0,137	1,81	0,036
<i>Profile V</i> Between latitude 36° to 47°S, longitude 73° and 90°W.											
45											
46	24,71	1,09	0,023	0,62	0,012	0,52	0,010	0,24	0,005	0,10	0,002
47	113,67	0,23	0,005	0,16	0,003	0,11	0,002	0,04	0,001	0,01	0,0001
48	153,56	0,22	0,004	0,17	0,003	0,12	0,002	0,06	0,001	0,03	0,001
49	160,80	0,29	0,006	0,23	0,005	0,20	0,004	0,10	0,002	0,03	0,001
50	96,80	0,06	0,001	0,04	0,001	0,07	0,001	0,07	0,001	0,03	0,001
51	80,80	0,62	0,012	0,09	0,002	0,11	0,002	0,09	0,002	0,02	0,0004
52	80,80	0,04	0,001	0,04	0,001	0,04	0,001	0,02	0,0004	0,01	0,0002
53	40,00	13,52	0,026	22,54	0,431	25,54	0,501	7,51	0,015	3,00	0,060
<i>Profile VI</i> In latitude 18°30'S.											
44											
45	57,28	3,46	0,069	3,87	0,077	4,28	0,086	4,28	0,086	3,06	0,061
46	57,72	1,82	0,036	7,88	0,158	9,50	0,180	9,10	0,172	6,47	0,129
47	58,16	0,80	0,016	1,20	0,024	0,40	0,008	0,60	0,012	0,60	0,012

Table 1 (continued)

St. No.	Surface level			Level of 50m		Level of 100 m		Level of 200 m		Level of 300 m	
	Milles [★]	V. c/s [#]	V. N. ^x	V. c/s	V. N.	V. c/s	V. N.	V. c/s	V. N.	V. c/s	V. N.
<i>Profile VII</i> In latitude 20°S.											
48											
49	58,61	7,38	0,148	6,46	0,129	7,94	0,159	7,01	0,140	4,25	0,085
50	58,61	4,80	0,096	4,43	0,089	4,25	0,085	3,51	0,070	2,58	0,052
51	58,61	2,95	0,058	2,22	0,044	0,19	0,004	0,55	0,011	0,55	0,011
<i>Profile VIII</i> In latitude 25°S.											
52											
53	55,20	4,76	0,095	9,67	0,183	10,94	0,208	10,47	0,199	9,04	0,170
54	55,20	6,34	0,127	3,65	0,073	0,95	0,018	1,27	0,025	1,11	0,022
55	54,00	6,16	0,123	5,51	0,110	2,76	0,055	0,49	0,009	1,46	0,029
<i>Profile IX</i> In latitude 30°S.											
56											
57	54,00	8,91	0,173	9,45	0,179	11,65	0,223	6,03	0,121	2,33	0,047
58	53,60	1,66	0,033	4,69	0,094	8,70	0,174	5,80	0,116	1,93	0,039
<i>Profile X</i> In latitude 30,5'S.											
101											
102	26,00	8,36	0,167	5,49	0,109	3,92	0,078	0,52	0,010	0,52	0,010
103	26,00	19,34	0,377	14,63	0,283	8,10	0,162	2,35	0,047	1,05	0,021
104	26,00	2,35	0,047	3,14	0,063	3,66	0,073	3,14	0,063	2,09	0,042
105	26,00	7,58	0,152	5,23	0,105	5,23	0,105	4,70	0,094	3,14	0,063
106	26,00	2,61	0,052	8,36	0,167	11,50	0,220	13,06	0,251	8,36	0,167
<i>Profile XA</i> In latitude 33°05'S.											
3											
4	52,00	9,41	0,178	6,66	0,133	4,31	0,086	1,70	0,034	0,52	0,010
5	44,00	7,10	0,142	4,32	0,086	2,47	0,049	1,08	0,022	0,15	0,003
6	60,00	1,13	0,023	1,25	0,025	0,79	0,016	0,57	0,011	0,45	0,009
7	41,20	2,47	0,049	2,31	0,046	3,79	0,076	5,94	0,119	5,11	0,102
<i>Profile XI</i> In latitude 40°S.											
94											
95	51,60	7,62	0,152	6,87	0,137	5,25	0,105	3,37	0,067	1,87	0,037
<i>Profile XII</i> No data available											
<i>Profile XIII</i> In latitude 47°S.											
66											
67	45,18	13,44	0,259	10,64	0,203	8,18	0,164	4,71	0,094	3,36	0,067
68	45,89	20,51	0,400	15,22	0,294	11,58	0,222	6,29	0,126	3,53	0,071

(★) Distance between oceanographic stations

(#) Velocity per cm/sec. between stations

(x) Velocity per knot/sec. between stations.

Table 2. Rainfall registered between Ancud and Cape Raper, from 1963 to 1968.

Year	1963	1964	1965	1966	1967	1968	Total Quarter	Aver. quart.	Total Years	Media Aver. Years
Ancud (Lat.41°54'S-Long. 73°48'W)										
1° Quarter	268,7	423,0	404,0	352,0	430,0	—	1.877,7	375,5		
2°	341,1	726,0	921,7	1.286,0	734,0	—	4.008,8	801,7		
3°	488,3	781,0	845,4	640,0	922,0	—	3.676,7	735,3		
4°	362,7	254,0	433,1	398,1	543,0	—	1.990,9	398,1	11.554,1	2.310,8
Total Year	1.460,8	2.184,0	2.604,2	2.676,1	2.629,0	—				
Castro (Lat. 41°54'S-Long. 73°48'W)										
1° Quarter	320,0	315,0	247,0	269,0	335,0	220,2	1.706,2	284,3		
2°	660,0	551,0	937,0	1.293,0	596,0	250,7	4.287,7	714,6		
3°	770,0	783,0	808,3	582,0	879,0	605,7	4.428,0	738,0		
4°	248,0	267,0	430,3	322,0	374,0	434,5	2.075,8	345,9		
Total Year	1.998,0	1.916,0	2.422,6	2.466,0	2.184,0	1.511,1			12.497,7	2.082,9
Quellón (Lat. 43°10'S-Long. 73°43'W)										
1° Quarter	—	366,0	406,3	—	437,0	414,2	1.623,5	405,8		
2°	—	617,0	802,8	—	942,0	494,3	2.856,1	714,0		
3°	—	729,0	1.044,8	—	1.022,0	1.009,5	3.805,3	951,3		
4°	—	302,0	657,6	—	520,0	895,1	2.374,7	593,6		
Total Year		2.014,0	2.911,5	—	2.921,0	2.813,1			10.659,6	2.664,9
Isla Guafo (Lat. 43°34'S-Long. 74°08'W)										
1° Quarter	98,5	204,0	201,1	150,0	197,0	—	850,6	170,1		
2°	469,6	248,0	442,1	592,0	236,0	—	1.987,7	397,5		
3°	524,4	—	334,4	190,0	246,0	—	1.294,8	258,9		
4°	159,6	260,0	194,3	197,0	196,0	—	1.006,9	201,3		
Total Year	1.252,1	712,0	1.171,9	1.129,0	875,0	—			5.140,0	1.028,0
Pto. Aysén (Lat. 45°24'S-Long. 72°42'W)										
1° Quarter	523,0	855,0	607,2	375,0	500,0	617,1	3.477,3	579,5		
2°	1.253,0	868,0	998,8	1.175,0	876,0	494,5	5.665,3	944,2		
3°	777,6	906,0	879,3	732,0	980,0	993,4	5.268,3	878,0		
4°	608,0	580,0	956,9	755,0	709,0	484,5	4.093,4	682,2		
Total Year	3.161,0	3.209,0	3.442,2	3.037,0	3.065,0	2.589,5			18.504,3	3.084,0
Cabo Raper (Lat. 46°50'S-Long. 75°36'W) 1°										
1° Quarter	181,2	257,0	199,6	258,0	250,0	302,5	1.448,3	241,3		
2°	308,9	253,0	303,0	386,0	364,0	250,8	1.865,7	310,9		
3°	288,0	268,0	217,2	211,0	239,0	275,4	1.498,6	249,7		
4°	220,2	218,0	162,6	—	305,0	360,7	1.266,5	211,0		
Total Year	998,3	996,0	882,4	855,0	1.158,0	1.189,7			6.079,1	1.013,1

The summer distribution of tuna in relation to the general oceanographic conditions off Chile and Peru

Table 3. Average catch in tons per degree of longitude and latitude, considering a longitude of 90° to 100°W (1963-1967)

Lat.	Bigeye	Yellowfin	Albacore	Stripped marlin	Total
4-5N	190.4	138.0		162.5	490.9
-4	476.0	96.6		110.5	683.1
-3	461.7	41.4		474.5	977.6
-2	390.3	34.5		539.5	964.3
0-1	366.5	51.8		533.0	951.3
0-1 S	409.7	110.8		97.5	618.0
-2	771.2	146.2		58.5	975.9
-3	886.9	168.3		71.5	1126.7
-4	376.0	234.3		55.3	665.6
-5	192.8	345.5		19.5	557.8
-6	303.7	354.4		39.0	697.1
-7	395.2	403.1		102.0	900.3
-8	395.2	121.8		89.1	606.1
-9	318.1	177.2		118.9	622.3
-10	313.3	73.9		260.0	647.2
-11	464.6	50.3		268.5	783.4
-12	328.3		3.04	260.0	591.34
-13	277.8	44.7	1.35	598.0	921.85
-14	328.3	36.7	1.69	702.0	1068.69
-15	464.6		13.5	455.0	933.1
-16	464.6	87.3	112.0	312.0	975.9
-17	328.3	85.5	141.6	279.5	834.9
-18	308.1	57.6	306.6	221.0	893.3
-19	388.9	82.6	152.1	97.5	721.1
-20	313.1	82.6	80.3	222.9	698.9
-21	702.0	34.7	34.5	371.5	1132.7
-22	459.0			408.8	867.6
-23	226.8	296.4	43.1	315.7	882.0
-24	135.0	148.2	28.8	260.0	572.0
-25				74.29	74.29
-26	189.0	395.2	57.5	371.5	1013.2
-27	286.2	164.5	26.5	267.4	744.6
-28	216.0	172.9	5.75	148.6	543.25
-29					
-30	594.0	49.4	361.5		999.9
-31	54.0		333.5	222.8	610.3
-32	432.0	263.3	34.5		729.8
-33	162.0		287.5	371.5	821.0
-34	216.0		57.5		273.5
-35	216.0		207.0		423.0
-36	216.0		402.5	96.6	715.1
-37	54.0		272.2		326.2
-38	270.0		218.5		488.5
-39			115.0		115.0
-40			126.5		126.5